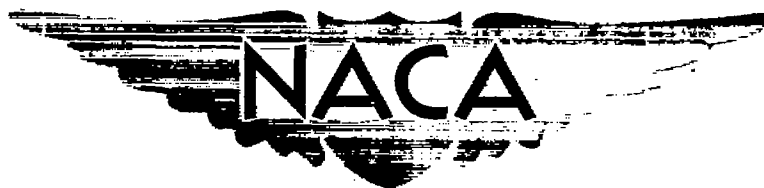


~~CONFIDENTIAL~~ UNCLASSIFIED

Copy *CV* 6
RM A55K01

NACA RM A55K01



RESEARCH MEMORANDUM

A FLIGHT EVALUATION OF A WING-SHROUD-BLOWING BOUNDARY-
LAYER CONTROL SYSTEM APPLIED TO THE FLAPS
OF AN F9F-4 AIRPLANE

By L. Stewart Rolls and Robert C. Innis

Ames Aeronautical Laboratory
Moffett Field, Calif.

CLASSIFICATION CHANGED

UNCLASSIFIED

To

By

authority of *Mem TPA 9* Date *6-1-59*
DB 11-23-59

RECEIVED
JAN 14 1959

LANGLEY AERONAUTICAL LABORATORY
LIBRARY, NACA
LANGLEY FIELD, VIRGINIA

CLASSIFIED DOCUMENT

This material contains information affecting the National Defense of the United States within the meaning of the espionage laws, Title 18, U.S.C., Secs. 793 and 794, the transmission or revelation of which in any manner to an unauthorized person is prohibited by law.

NATIONAL ADVISORY COMMITTEE FOR AERONAUTICS

WASHINGTON

February 14, 1958

~~CONFIDENTIAL~~

UNCLASSIFIED



UNCLASSIFIED

NATIONAL ADVISORY COMMITTEE FOR AERONAUTICS

RESEARCH MEMORANDUM

A FLIGHT EVALUATION OF A WING-SHROUD-BLOWING BOUNDARY-
LAYER CONTROL SYSTEM APPLIED TO THE FLAPS
OF AN F9F-4 AIRPLANE

By L. Stewart Rolls and Robert C. Innis

SUMMARY

As a portion of the general research program on the use of boundary-layer control to improve the maximum lift characteristics of airplane wings, the Bureau of Aeronautics loaned the Ames Aeronautical Laboratory of the NACA an F9F-4 airplane to evaluate a high-energy blowing boundary-layer-control system in flight. The high-energy blowing-boundary-layer control system was installed in the F9F-4 airplane by the Grumman Aircraft Engineering Corporation on contract with the Bureau of Aeronautics.

A series of test flights were made to measure the lift and drag variations with changes in angle of attack for the flap and gear both up and down and for blowing both on and off. The test data indicated that the boundary-layer-control system increased the maximum lift coefficient in the approach configurations from 1.98 to 2.32. An evaluation of the airplane by the four research pilots at the Laboratory indicated an average reduction of 10 knots in the approach speed by the use of the boundary-layer-control system. Calculations were made to evaluate the performance capabilities of the airplane with boundary-layer control in the take-off, catapult, approach, and landing configurations.

INTRODUCTION

An increased emphasis has been placed, in the last few years, on the use of boundary-layer control (BLC) to improve the lift characteristics of wings. Research studies on the use of boundary-layer control have been conducted by the Air Force, the Bureau of Aeronautics, universities, and the National Advisory Committee for Aeronautics. This research has been conducted with both area-suction (e.g., ref. 1) and high-energy blowing (e.g., ref. 2) types of boundary-layer control.

~~CONFIDENTIAL~~

UNCLASSIFIED

As a portion of this extensive program, the Bureau of Aeronautics contracted with the Grumman Aircraft Engineering Corporation to modify an F9F-4 airplane to incorporate a high-energy blowing system over the flap. The Bureau of Aeronautics loaned this boundary-layer-control equipped F9F-4 to the Ames Aeronautical Laboratory of the NACA to evaluate the boundary-layer control system in flight.

The purpose of this report is to present the in-flight evaluation of the high-energy boundary-layer control system, to compare the present results with those derived from small-scale wind-tunnel tests, and to calculate the effect of the use of the boundary-layer control system on the landing and take-off characteristics based on the flight results of the aircraft.

NOTATION

C_D drag coefficient, $\frac{\text{drag}}{qS}$

C_L lift coefficient, $\frac{\text{lift}}{qS}$

$C_{L_{\max}}$ maximum lift coefficient

c_p specific heat at constant pressure

C_μ momentum coefficient, $\frac{wV_j}{Sgq}$

F_G gross thrust, lb

g acceleration constant, 32.2 ft/sec²

J mechanical equivalent of heat, ft-lb/Btu

N engine speed, percent

p_d duct static pressure, lb/sq ft

p_o free-stream static pressure, lb/sq ft

q dynamic pressure, lb/sq ft

S wing area, sq ft

T_d	air temperature in duct, °R
V_j	velocity of blowing jet, assuming isentropic expansion to free-stream static pressure, $\sqrt{2gJc_pT_d\left(1 - \frac{p_o}{p_d}\right)^{0.286}}$, ft/sec
w	weight flow of air in the blowing system, lb/sec
x	horizontal distance from the nozzle to the tangent point on the flap nose, in.
y	vertical distance from nozzle to the tangent point on the flap nose, in.
α	angle of attack, deg
ΔC_L	increment between two values of C_L at constant angle of attack
δ	ratio of total pressure at compressor to total pressure at sea level
θ	ratio of total temperature at compressor to total temperature at sea level

AIRPLANE AND INSTRUMENTATION

The airplane used in these tests, a Grumman F9F-4, is a single-place, straight-wing, jet-propelled aircraft. A drawing of the test airplane is shown in figure 1 and a photograph in figure 2. Dimensional data for the airplane are presented in table I. External modifications made to the airplane consisted of a nose boom used to mount an airspeed head and an angle-of-attack vane. During this investigation the gross weight of the airplane varied from 15,000 pounds to 13,000 pounds and the center of gravity was at about 24 percent of the mean aerodynamic chord.

The entire boundary-layer control system was installed by the Grumman Aircraft Engineering Corporation. A schematic drawing of this system is shown in figure 3. The system consists of ports on the engine, the ducting from the engine to the flap, the blowing slit over the flap, and a control valve actuated manually by the pilot. A sketch of the wing cross section showing the relative location of the wing duct, nozzle in the wing shroud, and flap is shown in figure 4(a). The variation of flap gap and flap spacing is shown in figure 4(b), and a photograph of the nozzle is shown in figure 4(c). The maximum air flow is governed by the nozzle exit area (2.6 sq in.) and the engine pressure since the wing

duct nozzles operate at a supercritical pressure. The variation of engine bleed air with engine speed, with the valve full open, is shown in figure 4(d). A nearly continuous nozzle was provided by the use of shims located every 1.5 inches spanwise which resulted in a mean nozzle gap of 0.040 inch as compared to a design value of 0.042 inch. The flaps-down tests were carried out with flaps deflected to 45° .

The normal flap system on the F9F-4 airplane consists of two flaps: a simple split flap located in the wing center section on the lower surface of the fuselage, and a slotted flap located on the inboard end of the wing outer panel. These two flaps are shown in figure 2. The blowing-system modifications were made to the wing ahead of the slotted flap only. These modifications consisted of relocating the flap hinge point to an optimum flap position for blowing, as indicated by wind-tunnel tests for this configuration (ref. 3), and also a redesign of the slotted-flap leading edge to form a converging channel between the relocated flap and the wing duct. The revised hinge fittings and flap actuators were mounted externally as shown in figure 5. The pylons which appear in this figure were not on the wing during the majority of these tests. The original droopable leading edge of the wing which is activated by the wing flap was maintained on this airplane.

Instruments were installed to simultaneously record measurements of airspeed, altitude, normal acceleration, longitudinal acceleration, angle of attack, and net thrust in order to determine the lift capabilities of the various configurations of the blowing system tested. Further instrumentation was installed in the airplane to measure the quantity of bleed air flow and the bleed duct pressure ratio.

TESTS

Measurements of the low-speed characteristics of the test airplane were taken at an altitude of 5,000 feet to permit complete stalling of the airplane without undue hazard. The data included in this report were taken during runs in steady flight at gradually decreasing airplane velocity, beginning at the placard speed with the flaps and gear down (220 knots), and continuing until about 10 knots above the stall speed. A time-history record was then obtained from this point down to the stall. The rate of change of airspeed during the time-history portion of the record did not exceed 1 knot per second. The records were terminated when the pilot felt the airplane was no longer controllable. The variations of flap effectiveness with momentum coefficient were obtained from data taken at various engine speeds and valve positions.

An appraisal of the boundary-layer control system, as installed in the F9F-4 airplane was made by the four research pilots at the Laboratory during simulated carrier landings, with a landing signal officer, with the boundary-layer control system on and off.

RESULTS AND DISCUSSION

Effect of Blowing on the Aerodynamic Characteristics

The configuration of the test airplane which will be considered as the basic configuration is shown in figure 2. This configuration was with tip tanks on, both the wing flap and the fuselage split flap operating, droopable nose activated by the flap, and the under surface of the wing clean except for the external hinges.

Lift and drag.- A set of data obtained for the test airplane in the approach condition is shown in figure 6. This figure shows the variation of angle of attack and drag coefficient with lift coefficient. The equations used to determine the lift and drag coefficients are discussed in Appendix A. Examination of these equations indicates that the lift and drag coefficients as presented in this report have been corrected for the effect of the engine thrust. The three airplane configurations for which data are presented in figure 6 are: (1) flaps and gear up, boundary-layer control off; (2) flaps and gear down, boundary-layer control off; and (3) flaps and gear down, boundary-layer control on. These data are for a flap deflection of 45° and an approach power setting of 85 percent of maximum engine speed. The difference in the angle of attack for stall with the flaps and gear up and with the flaps and gear down is attributable, in part, to the droopable leading edge which is deflected when the trailing-edge flap is lowered. The maximum lift coefficients shown in this figure are 1.30 flaps and gear up, 1.98 flaps and gear down - blowing off, and 2.32 flaps and gear down - blowing on.

Also shown in figure 6 is the variation of momentum coefficient (C_μ) with lift coefficient. This variation in momentum coefficient is the result of the gradual decrease in dynamic pressure used to vary the lift coefficient during a test run.

Comparison of the drag polars shown in figure 6 indicates that the drag coefficients with blowing on are greater than with blowing off at low values of lift coefficients. This was also indicated in the wind-tunnel tests of this installation (ref. 3). These higher drags are attributed to the increase in the induced drag caused by changes in the span load distribution as a result of the blowing over the flap. The method of references 4 and 5 was used to compute the theoretical increase in the induced drag. The computed increase was approximately 0.025 which compares with a measured increase of approximately 0.030, thus indicating that the measured increment is slightly greater than that computed by theory.

Effect of changing engine speed.- To evaluate the effect of changing the engine speed as might occur during a take-off or a wave-off maneuver, the lift and drag characteristics of the airplane were measured

at military power (100-percent rpm). These lift and drag variations, along with the variation in momentum coefficient, are presented in figure 7. Also shown in this figure are the characteristics measured at the approach power ($N = 85$ percent). These data show that at military power, the lift coefficient is higher for the same angle of attack and the drag coefficient is higher for the same lift coefficient. These changes are attributed to increases in momentum coefficient at the higher engine speed and will be discussed more fully in a later section.

Effect of Blowing on Lift Increments

The variation of airplane lift coefficient with momentum coefficient at several values of angle of attack is presented in figure 8. The change in flap lift increment with changes in momentum coefficient at constant angle of attack is presented in figure 9. These data indicate that the lift increment due to blowing approaches a constant value at the higher values of momentum coefficient at angles of attack below that for maximum lift.

To evaluate the effectiveness of the boundary-layer control system, a comparison was made between the flap lift increments obtained during flight and the theoretical flap lift increments computed by the method of reference 5. A comparison is presented in figure 10. The airplane configuration used in this comparison was selected as one on which the flap lift increment could be most reliably computed by means of the theory (i.e., blowing flap deflected, split flap retracted, nose flap locked drooped, and wing tip tanks removed). The flap lift increments, as shown in this figure, are larger than those computed from reference 5. The exact breakdown of these higher lifts between circulation increases and mere momentum changes is unknown; however, assuming the total momentum of the blowing system was converted into lift, due to its downward deflection, the lift coefficient would be increased by only 0.022. A photograph of the airplane as modified to obtain the data to correlate with the theory is shown in figure 11. The measured lift coefficients versus angle of attack for this configuration are shown in figure 12.

A comparison of the flight results with the results of a 1/5.5-scale model of the F9F-4 performed at the David Taylor Model Basin (ref. 3) is presented in figure 13. In figure 13(a) the comparison of the flight and tunnel measured variation of lift coefficient with angle of attack is presented. The variation as measured in the wind tunnel as shown in this figure has been corrected for the same variation in momentum coefficient as occurred during a typical flight data run. This comparison indicates a higher flight lift coefficient than measured in the wind tunnel. The difference in angle of attack for stall as measured in the wind tunnel must be attributed to Reynolds number as there was no difference in model configuration indicated. A comparison of the increment in lift due to

blowing is presented in figure 13(b). It was necessary to base this comparison on the increment due to blowing as there were no data available from which to compute the effectiveness of the basic flap of the wind-tunnel model. This comparison also shows that the lift increments as measured in flight are higher than those indicated by the wind-tunnel tests. These wind-tunnel data show the same tendency as the flight data to level off at the higher values of momentum coefficient. The lower lift increments due to blowing measured in the tunnel may be the result of a more effective basic flap installation on the model (i.e., no cut-outs, no external hinges, and a smoother surface) than was present on the test airplane.

Effect of Blowing on the Take-Off and Landing Characteristics

In order to operate the engine in the F9F-4 airplane during blowing operation without exceeding the limits of tail pipe temperature, it was necessary to increase the area of the tail pipe exit. This modification to the engine tail pipe resulted in a thrust loss on the modified engine. Figure 14, based on the data from reference 6, shows the thrust variation with engine speed for the engine as modified to include the blowing system, and for comparison the thrust variation of an unmodified engine is also shown. Whether the blowing system was operating or not did not appreciably affect the thrust characteristics of the modified engine. To evaluate the effect of these losses in thrust on the performance of the airplane, comparisons will be made in the following conditions: (a) take-off, (b) catapult take-off, (c) approach, and (d) landing. The methods used to compute these values are presented in Appendix B. Since the take-off speed and the catapult speed are set up as functions of $C_{L_{max}}$, or the stalling speed, these speeds are presented in figure 15 for comparison.

Take-off characteristics.- From the take-off speeds as defined in figure 15 the following take-off distances have been computed:

	Weight = 15,000 lb		Weight = 18,000 lb	
	Ground run	Distance over 50 foot obstacle	Ground run	Distance over 50 foot obstacle
Blowing on	1805	2729	2910	4160
Blowing off	2113	3135	3410	4755
Standard airplane	1654	2590	2595	3679
Blowing on (assuming no thrust losses)	1396	2217	2190	3245

It will be noted that the airplane is critically affected by the loss of thrust caused by the installation of the blowing system; in fact, it cancels any benefit which might be derived from the blowing system. If the blowing system could be installed without these severe thrust losses, appreciable gain in the take-off performance could be realized.

Catapult take-off characteristics.- Since the land take-off is only one phase of the take-off problem, an estimate of the catapult capabilities of the airplane was made. The catapult end speeds for the airplane with blowing on and the standard airplane are shown in figure 15. Also shown in this figure is the capability of an H4B catapult. The abrupt termination of the catapult end speed curve for the airplane with boundary-layer control, at a gross weight of 19,700 pounds, is caused by the fact that the excess thrust (thrust available minus thrust required) no longer exceeds an assumed minimum desirable value of 0.065 times the gross weight. The difference between the velocity supplied by the catapult and the end speed required is the amount of wind that has to be blowing over the deck. The wind over the deck required as a function of the gross weight for the two airplane configurations is presented in figure 16. It will be noted, at weights below 19,700 pounds, that the airplane with boundary-layer control requires about 6 knots less wind than the standard airplane.

Approach characteristics.- Based on an evaluation by the four research pilots (which will be discussed in the next section), the approach speeds were 103 knots with the standard airplane and 93 knots with the boundary-layer control system operating. These speeds are based on a gross weight of 13,100 pounds. If the approach lift coefficients are plotted on the lift curves for the basic configuration as is done on figure 17, it is seen that the effect of operating boundary-layer control systems is to allow the pilot to approach at an angle of attack, blowing on, equal to or greater than that with blowing off. If it is assumed that the angle of attack will be kept constant then the variation of approach speed with gross weight can be computed. This variation is shown on figure 18.

Landing characteristics.- To evaluate the effect of the boundary-layer control system on the actual landing performance of the airplane the landing distances have been computed and are compared in the following table. To calculate this sinking type approach an engine speed of 70 percent and a $C_{L_{max}}$ with blowing on of 2.1 were used. During a landing the thrust loss on the airplane with boundary-layer control is no longer a factor and the benefit of the boundary-layer control is readily seen. In the calculations approach power is assumed until the touchdown point at which time a complete chop of power is made and no thrust acts during the ground run.

	Weight = 13,000 lb		Weight = 15,000 lb	
	Ground run	Distance over 50 foot obstacle	Ground run	Distance over 50 foot obstacle
Boundary-layer control on	1515	2560	1755	2730
Boundary-layer control off (or standard airplane)	1620	3680	1880	3440

Pilot's Opinion

A short evaluation of the airplane was conducted by four NACA pilots to determine the minimum safe speeds at which carrier-type approaches could be made with and without the boundary-layer control system. The speeds chosen by each pilot, as well as the reasons for choosing them, are shown in table II. These speeds are corrected to calibrated airspeed and correspond to a normal landing gross weight of approximately 13,100 pounds. Also included in this table is a summary of the stall speeds (corrected to calibrated airspeed) and stall characteristics of the airplane as reported by each pilot.

It will be noted that an appreciable difference exists between the approach speeds chosen by the different pilots. This can be attributed to the individual interpretation of a "minimum safe approach speed" and to the varying degrees of turbulence encountered by each pilot. Because of this, it is felt that a much more valid evaluation of the system can be obtained by comparing the decrease in approach speed experienced by each pilot due to the use of boundary-layer control rather than comparing the average approach speed. On the basis of this, it seems that an average of a 10-knot reduction in approach speed can be realized by the use of this system.

The primary reason for limiting the approach speed lies in the ability to control the airplane altitude or to arrest a sink rate. This speed seems to be that at which the pilot feels he can rotate the airplane to change his flight path angle by an adequate amount and still have sufficient thrust response from the engine to overcome the increased drag associated with the higher angle of attack. In only one case, that of the pilot who chose the lowest approach speed, was proximity to stall considered a limiting factor. The lift coefficients corresponding to each pilot's choice of approach speed are shown in figure 17. Included in this figure are the average values of lift coefficient computed from the approach airspeeds measured in reference 6. It should be noted that with this particular application of boundary-layer control the pilots

seem willing not only to use all of the lift increment provided by the system at a given angle of attack but, with the system operating, to increase slightly the angle of attack at which they approach.

The stall characteristics of the airplane are generally considered to range from marginal to unsatisfactory, due to the unacceptable roll-off which occurred at the stall. This roll-off seemed to be slightly more pronounced with the boundary-layer control on. Opinion was divided as to the adequacy of the stall warning; however, the consensus was that it was rather weak and occurred close to the stall.

The lateral-directional stability of the airplane in the approach configuration is poor and does not seem to be changed much by the application of boundary-layer control; though at the higher approach speeds, with the system operating, there is an apparent breakdown and reattachment of flow over portions of the flap which gives rise to rolling moments and further excites the lateral-directional oscillations.

As no quantitative measurements were made of the take-off performance of the airplane, the only data that can be given are a comparison of pilot opinion with and without the system operating. Some difficulty was experienced in obtaining nose wheel lift-off with the boundary-layer control on, due probably to the nose-down pitching moment associated with operating the system. The take-off was accomplished at a lower airspeed with the boundary-layer control on; however, the higher drag was quite noticeable to all the pilots and resulted in a lower acceleration, which partially canceled the effects of the decrease in take-off speed.

Other Configurations Tested

In addition to the data obtained for the basic configuration, certain other configurations were tested. The lift and drag data for these other configurations are presented in figures 19 through 21. The configurations were: (1) the basic configuration but with pylons mounted on the lower surface of the wing as shown in figure 5; (2) the basic configuration with the droopable leading edge of the wing locked down; and (3) the basic configuration with only the outboard flap deflected, but with the tip tanks on. The variations of momentum coefficient with lift coefficient during these test runs were similar to that shown in figure 6. A comparison of figures 20 and 21 indicates that the reduction in maximum lift coefficient from closing the split flap under the fuselage was about 0.13. A comparison of figures 19 and 20 indicates that reduction in the angle for maximum lift for the airplane with flaps and gear up could be attributed for the most part to the droopable leading edge.

CONCLUDING REMARKS

The in-flight evaluation of the high-pressure-blowing boundary-layer control system as installed in the F9F-4 airplane resulted in the following:

1. The use of blowing increased the maximum lift coefficient in the approach condition from 1.98 to 2.32.

2. The flap lift increment with blowing on was greater than the theoretical flap lift increment, so it was possible that some increase in circulation could be present with the boundary-layer control system operating.

3. The flight-test data indicate a larger favorable effect caused by the boundary-layer control system than that measured on a 1/5.5-scale model of the F9F-4 airplane in a wind tunnel.

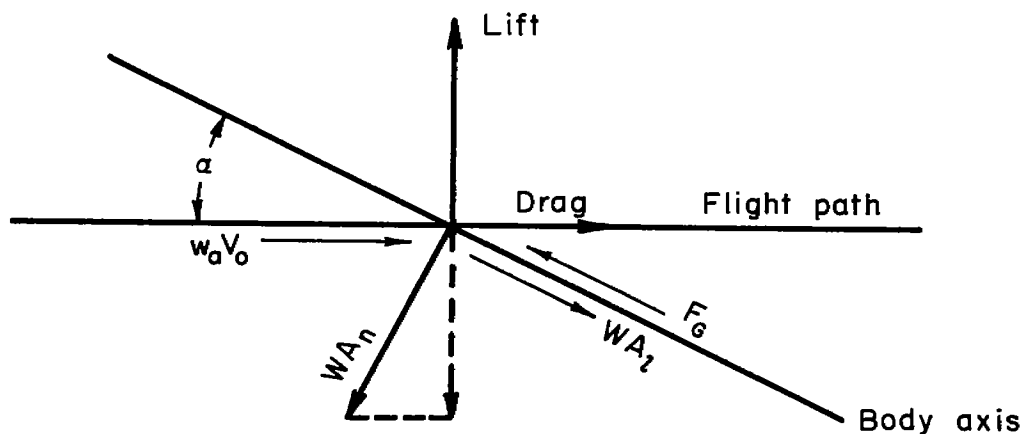
4. Calculations of the take-off distances showed little improvement for the boundary-layer control airplane, due to the thrust loss of the engine during blowing operation. The boundary-layer control airplane, however, could be catapulted successfully with less "wind over the deck" than the standard airplane.

5. The effect of operating with boundary-layer control is that it allows the pilot to approach at an angle of attack equal to or greater than that used without boundary-layer control. This corresponds roughly to a 10-knot reduction in the approach speed, due to operation of the boundary-layer control system.

Ames Aeronautical Laboratory
National Advisory Committee for Aeronautics
Moffett Field, Calif., Nov. 1, 1955

APPENDIX A

EQUATIONS USED FOR DETERMINING LIFT AND DRAG



With the notation and sign convention indicated in the above diagram, the lift and drag equations, as used in this report, are as follows:

$$\text{Lift} = W(A_n \cos \alpha + A_l \sin \alpha) - F_G \sin \alpha$$

$$\text{Drag} = W(A_n \sin \alpha - A_l \cos \alpha) + F_G \cos \alpha - w_a V_0$$

where

W weight of airplane, lb

A_n normal acceleration factor, g units

A_l longitudinal acceleration factor, g units

α angle of attack, deg

F_G gross thrust, lb

w_a engine inflow, slugs/sec

V_0 airplane free-stream velocity, ft/sec

The weight of the airplane was determined from the take-off weight and the amount of fuel used between the take-off and the time of the run.

A total-pressure probe was mounted in the tail pipe of the jet engine to give data for the determination of engine gross thrust and air flow. In order to use the data from a single probe, it was necessary to assume that a uniform distribution of temperature and pressure existed across the tail pipe. It was also assumed that the static pressure in the tail pipe exit was equal to free-stream static pressure and that there were no nozzle losses. The equations used for engine thrust and air flow determination are presented in reference 7.

APPENDIX B

METHODS USED TO EVALUATE THE PERFORMANCE CAPABILITIES
OF THE BOUNDARY-LAYER CONTROL SYSTEM

The following are the equations used and the assumptions made to calculate the performance capabilities of the boundary-layer control system on the F9F-4 airplane.

Take-off distance:

$$\text{Ground run} = \frac{WV_{TO}^2}{64.4[T - \mu W - qS(C_D - \mu C_L)]}, \text{ ft}$$

where the take-off velocity

$$\begin{aligned} V_{TO} &= 1.2 V_{\text{stall}} \\ &= 1.2 \left(1.837 \sqrt{\frac{W - T \sin \alpha}{C_{L_{\max}}}} \right), \text{ ft/sec} \end{aligned}$$

and

$$q = \frac{1}{2} \rho (0.7 V_{TO})^2$$

T = thrust at 100-percent N

W = gross weight in pounds

μ = 0.02

α = angle of attack corresponding to $C_{L_{\max}}$

Acceleration is assumed to vary linearly up to take-off velocity. On this aircraft the maximum ground angle is 12° so this value does not limit the take-off calculations (ref. 8, pp. 194-196).

$$\text{Air distance} = \frac{50 W}{T - D} + \frac{V_{TO}^2}{32.2\sqrt{2}}, \text{ ft}$$

where

D = drag at $0.7 C_{L_{\max}}$

In this equation it is assumed that thrust and drag remain constant during transition and that maximum steady climb has been reached before attaining the 50-foot height (ref. 9, pp. 48-51).

Landing distance:

$$\text{Ground roll} = \frac{V_L^2}{64.4 \left[\mu - \left(\frac{D}{L} \right) \right]} \log e \left(\frac{L\mu}{D} \right), \text{ ft}$$

where the landing velocity

$$V_L = 1.15 V_{\text{stall}}$$

and

$$\mu = 0.40$$

In this equation it is assumed that C_L is constant and there is no thrust during ground run (ref. 10, pp. 311-313).

$$\text{Air distance} = \left[\frac{(V_{50}^2 - V_L^2)}{64.4} + 50 \right] \frac{W}{D - T}, \text{ ft}$$

where the velocity at the 50-foot height

$$V_{50} = 1.2 V_{\text{stall}}$$

and

$$T = \text{thrust at 70-percent } N$$

(ref. 8, pp. 197-198).

Catapult end speed:

$$V_{TO} = \sqrt{\frac{295(W - T \sin \alpha)}{SC_{L_{TO}}}}, \text{ knots}$$

where

$$T = \text{thrust at 100-percent } N$$

$$C_{L_{TO}} = 0.9 C_{L_{\text{max}}}$$

$$\alpha = \text{angle of attack corresponding to } C_{L_{TO}}$$

REFERENCES

1. Cook, Woodrow L., Holzhauser, Curt A., and Kelly, Mark W.: The Use of Area Suction for the Purpose of Improving Trailing-Edge Flap Effectiveness on a 35° Sweptback Wing. NACA RM A53E06, 1953.
2. Kelly, Mark W., and Tolhurst, William J., Jr.: Full-Scale Wind-Tunnel Tests of a 35° Sweptback Wing Airplane With High-Velocity Blowing Over the Trailing-Edge Flaps. NACA RM A55I09, 1955.
3. Murphy, R. D., Harkleroad, E. L., and Barnard, G. A.: Wind-Tunnel Tests of a 1/5.5-Scale Model of an F9F-4 Airplane Incorporating High-Speed Air Ejection Over the Aft Section of the Wing. Aero. Rep. 873, TED No. TMB AD-3155, David Taylor Model Basin, Nov. 1954.
4. DeYoung, John, and Harper, Charles W.: Theoretical Symmetric Span Loading at Subsonic Speeds for Wings Having Arbitrary Plan Form. NACA Rep. 921, 1948.
5. DeYoung, John: Theoretical Symmetric Span Loading Due to Flap Deflection for Wings of Arbitrary Plan Form at Subsonic Speeds. NACA Rep. 1071, 1952.
6. Duerfeldt, C. H.: F9F-4 Airplane with Supercirculation Boundary-Layer Control; Performance, Flying Qualities, Landbased and Shipboard Carrier Suitability Evaluation, Letter Report No. 1, Final Report. Naval Air Test Center, Patuxent River, Md. Project TED No. PTR AD-349, June 2, 1954.
7. Rolls, L. Stewart, and Havill, C. Dewey: Method for Measuring Thrust in Flight on Afterburner-Equipped Airplanes. Aero. Engr. Rev., vol. 13, no. 1, Jan. 1954, pp. 45 - 49.
8. Perkins, Courtland D., and Hage, Robert E.: Airplane Performance Stability and Control. John Wiley and Sons, Inc., 1949.
9. Lush, Kenneth J.: Standardization of Take-Off Performance Measurements for Airplanes. Tech. Note R-12, Edwards Air Force Base, Edwards, Calif., 1954.
10. Dwinell, James H.: Principles of Aerodynamics. McGraw-Hill Book Company, Inc., 1949.

TABLE I.- DIMENSIONAL DATA FOR THE GRUMMAN F9F-4 AIRPLANE

Wing	
Airfoil section	NACA 64A010
Area, sq ft	250
Span, ft	38
Root chord, in.	117
Tip chord, in.	44
Mean aerodynamic chord, in.	89.5
Aspect ratio	5.0
Incidence, deg	0
Flaps	
Slotted	
Inboard end at 26.3-percent semispan	
Outboard end at 59-percent semispan	
Area, sq ft	33
Deflection, deg	45
Split (under fuselage)	
Inboard end at 0-percent semispan	
Outboard end at 26-percent semispan	
Area, sq ft	21.7
Deflection, deg	40
Nose	
Inboard end at 26.3-percent semispan	
Outboard end at 89.8-percent semispan	
Area, sq ft	25
Deflection, deg	19

TABLE II.- PILOTS' COMMENTS RELATING TO STALL AND APPROACH CHARACTERISTICS OF THE F9F-4
WITH BLOWING FLAP

Pilot	Configuration	Stall characteristics (power approach configuration)			Approach speed ¹	Primary reasons for choosing approach speed
		Airspeed	Gross Weight	Opinion		
A	Blowing off	Warn: 95 Stall: 90	14,700	Warn: Inadequate Stall: Marginal	107	Inadequate altitude control Inability to arrest sink rate
	Blowing on	Warn: 85 Stall: 82	14,700	Warn: Inadequate Stall: Marginal	96	Inadequate altitude control Inability to arrest sink rate
B	Blowing off	Warn: 93 Stall: 90	14,500	Warn: OK Stall: Marginal	103	Inadequate altitude control Lateral response and stability in gust
	Blowing on	Warn: 87 Stall: 82	14,400	Warn: OK Stall: Marginal	95	Inadequate altitude control Lateral response and stability in gust
C	Blowing off	Warn: 95 Stall: 92	14,700	Warn: Unsatisfactory Stall: Unsatisfactory	100	Inadequate longitudinal control response
	Blowing on	Warn: 88 Stall: 84	14,600	Warn: Marginal Stall: Unsatisfactory	91	Inadequate longitudinal control response
D	Blowing off	Warn: 90 Stall: 90	15,000	Warn: Satisfactory Stall: Satisfactory	100	Altitude control
	Blowing on	Warn: 80 Stall: 77	13,300	Warn: Unsatisfactory Stall: Unsatisfactory	88	Proximity to stall and altitude control

¹Airplane gross weight, 13,100 lb.

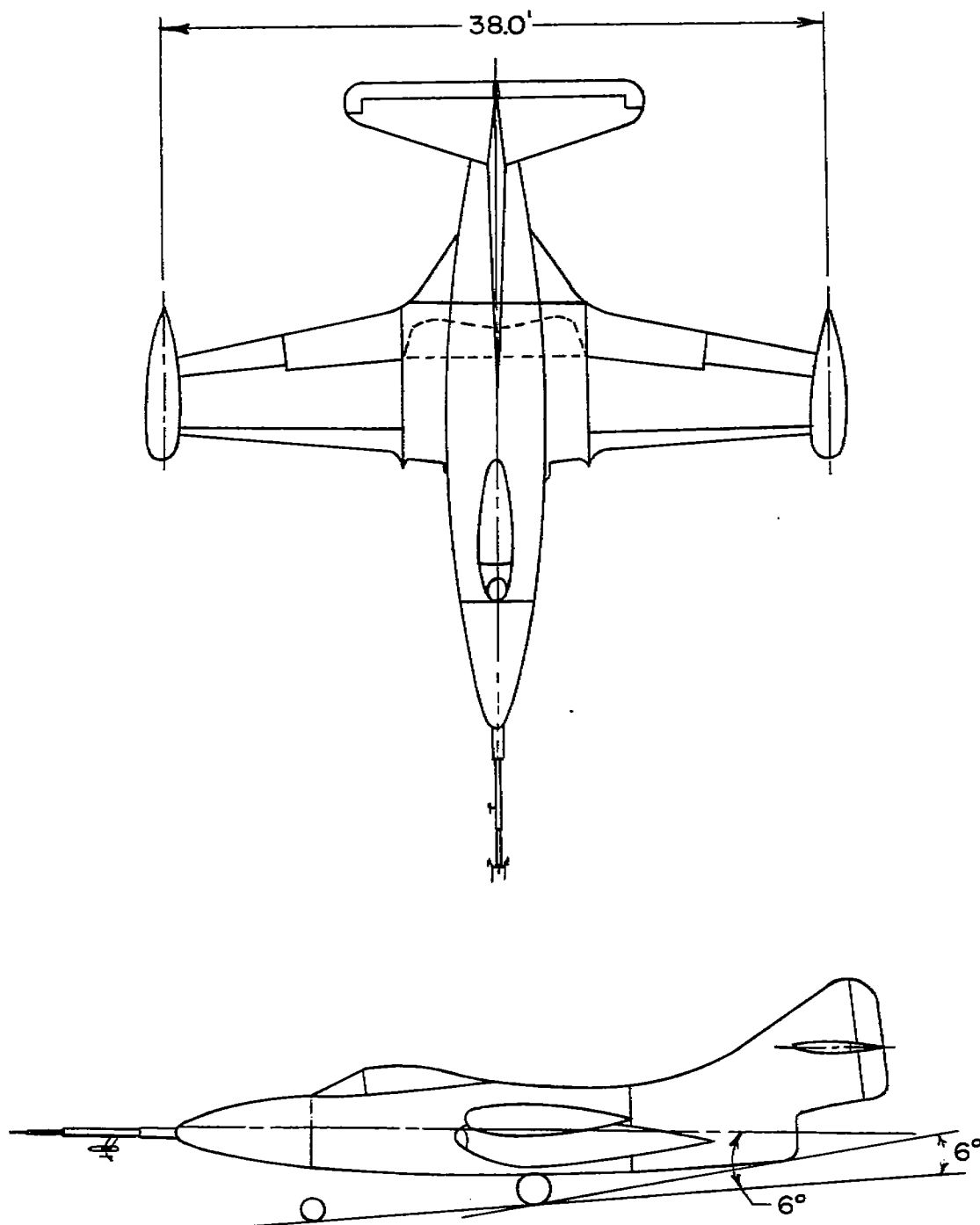


Figure 1.- Drawing of the test airplane.



(a) Flaps up.

A-10256

Figure 2.- Three-quarter rear view of test airplane.



(b) Flaps down.

Figure 2.- Concluded.

A-20257

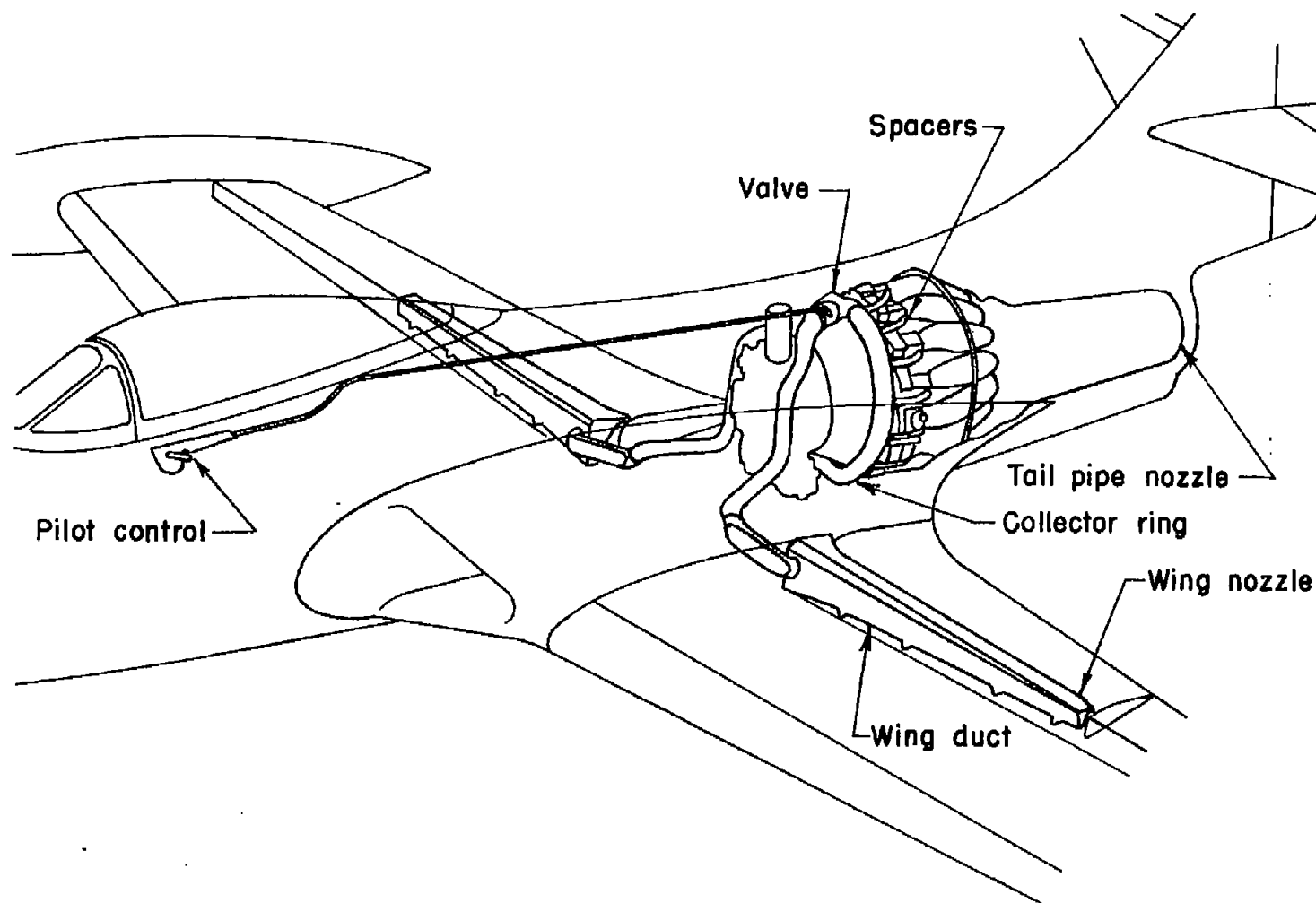
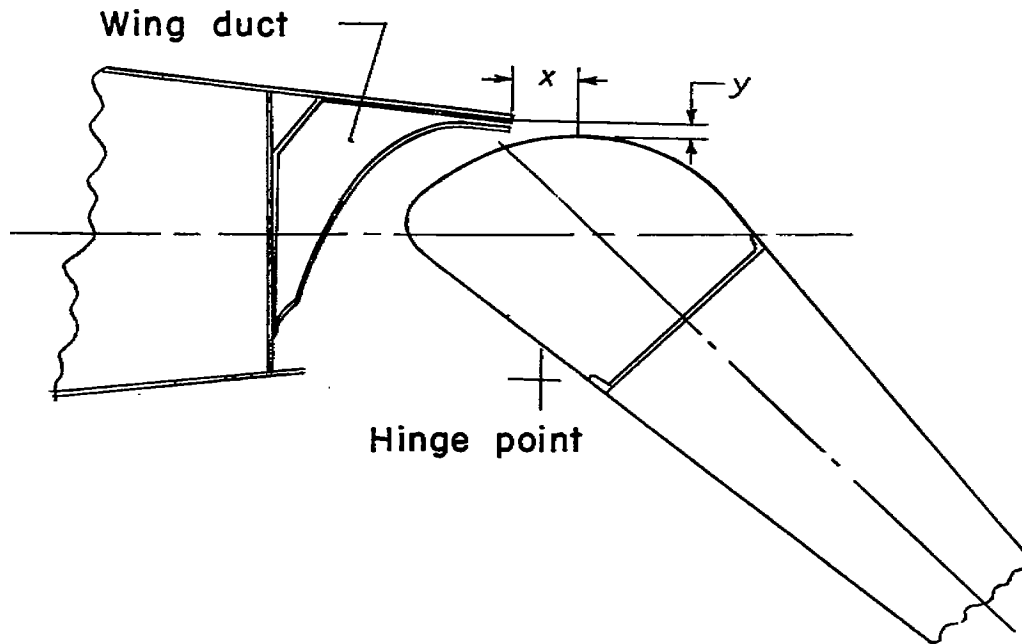
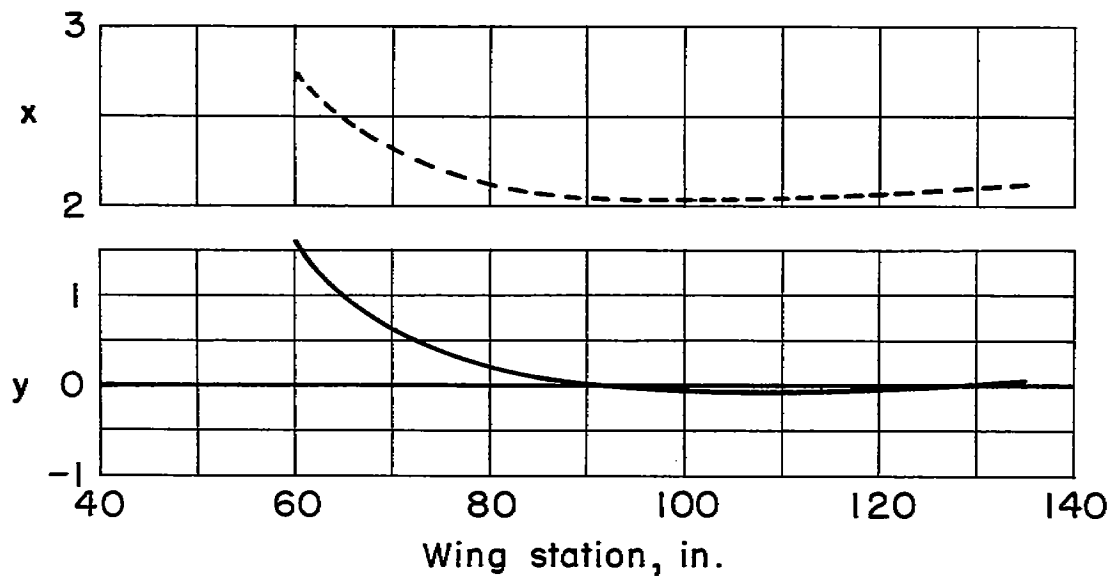


Figure 3.- Schematic drawing showing the wing-shroud-blowing system.

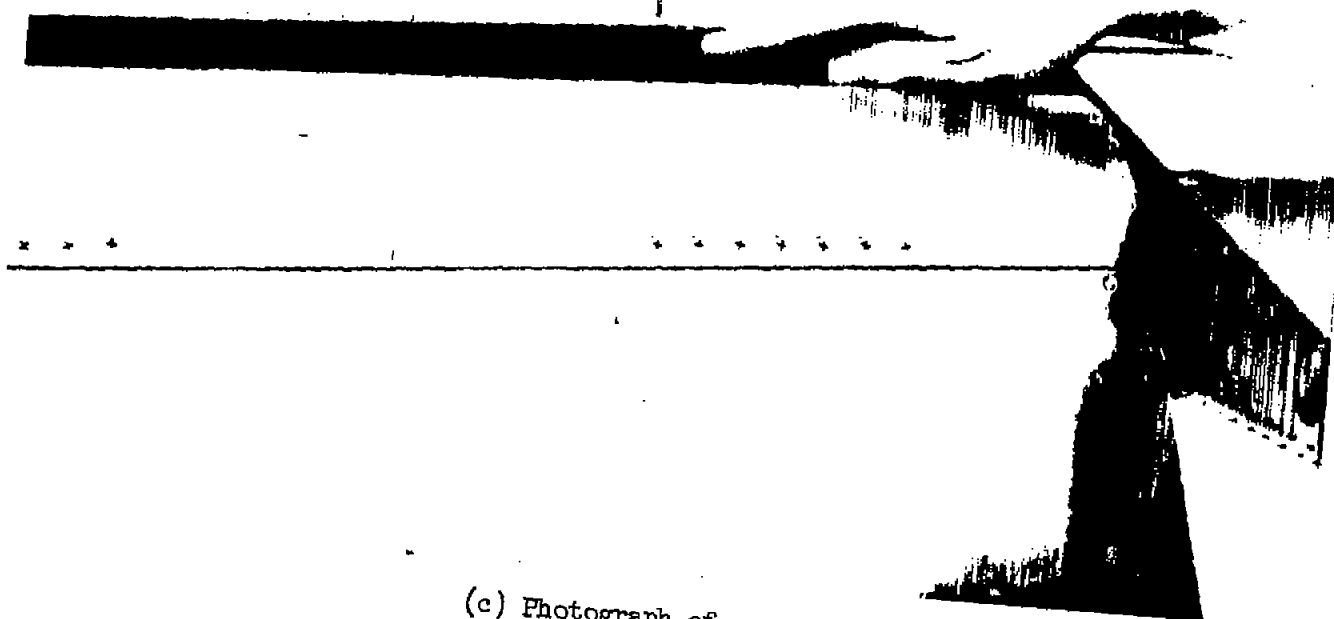


(a) Typical cross section of wing through the flap.



(b) Location of blowing nozzle with respect to the flap.

Figure 4.- Details of the blowing flap installation.

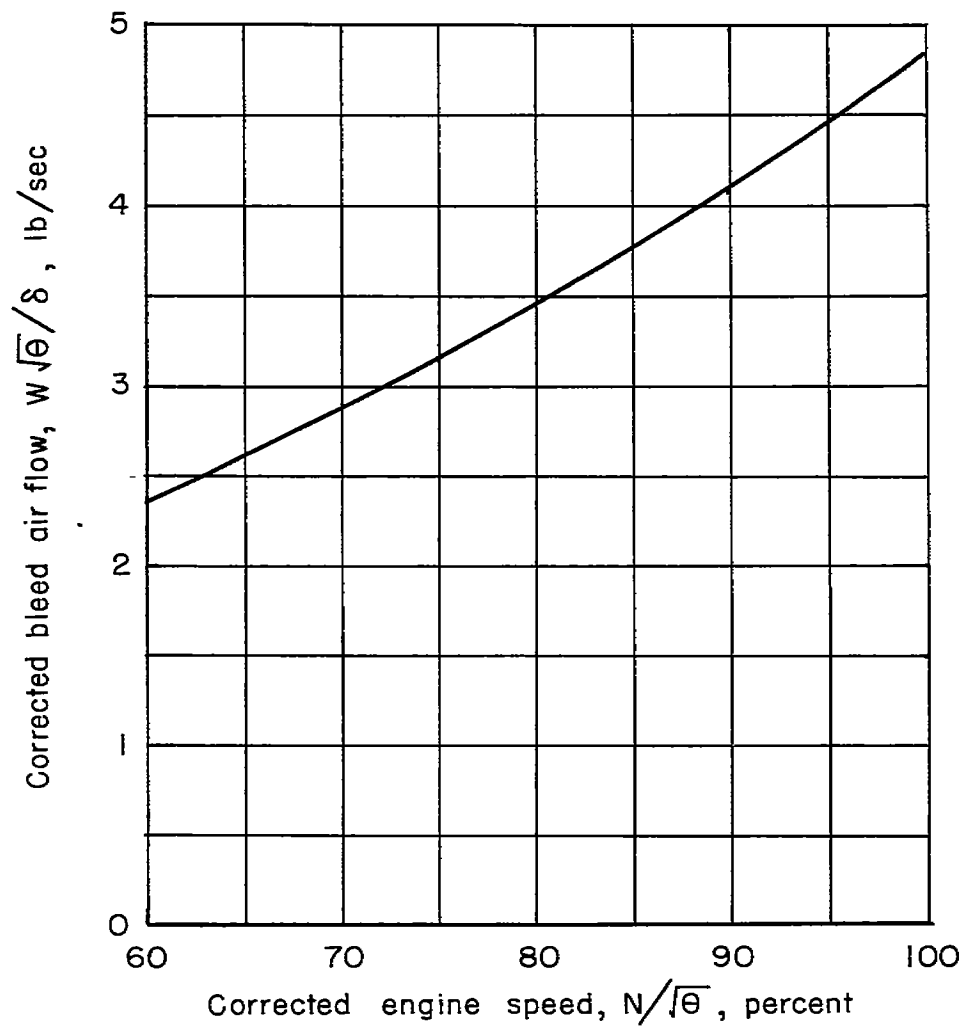


(c) Photograph of nozzle.

Figure 4.- Continued.

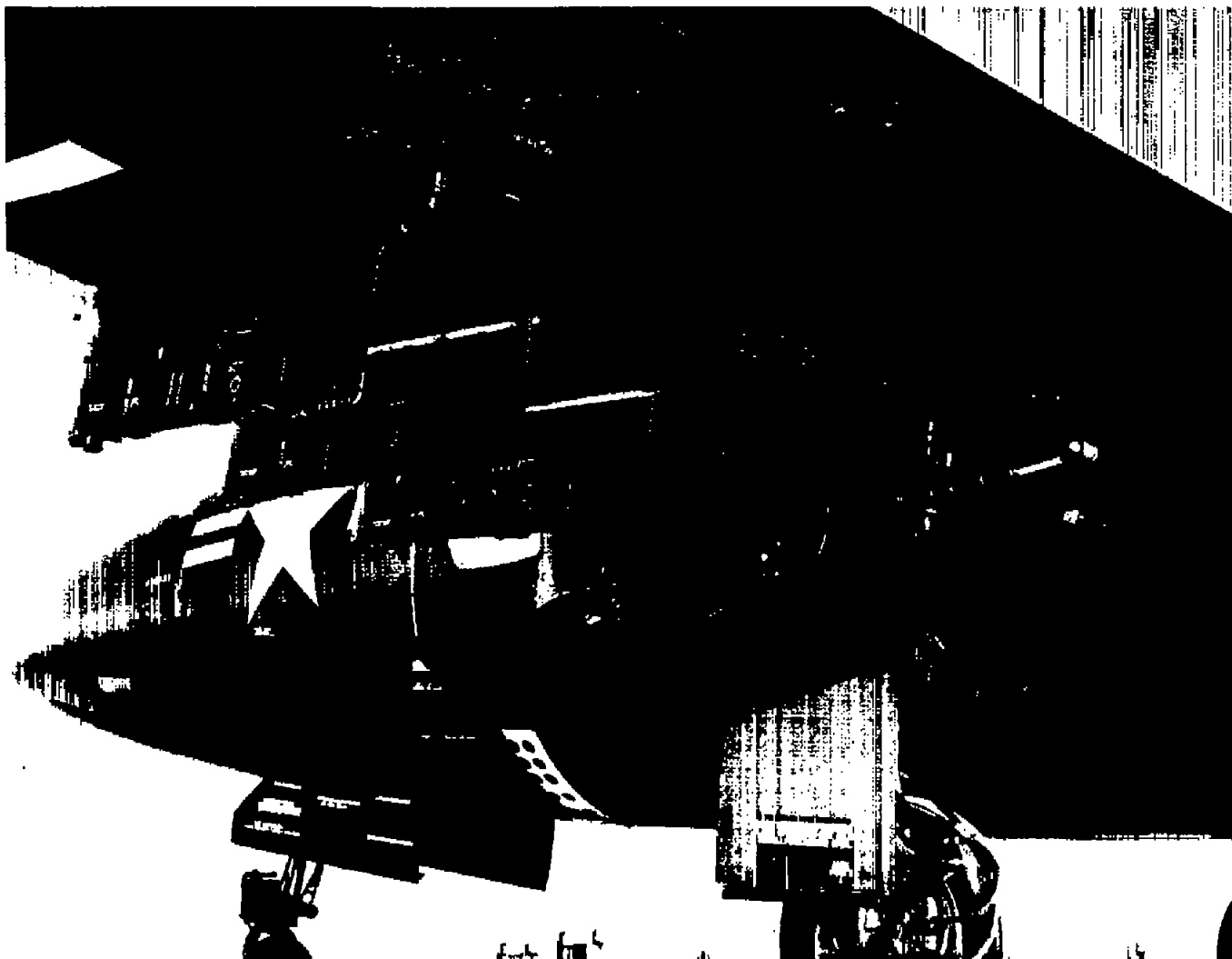
A-20258

NACA RM A55K01



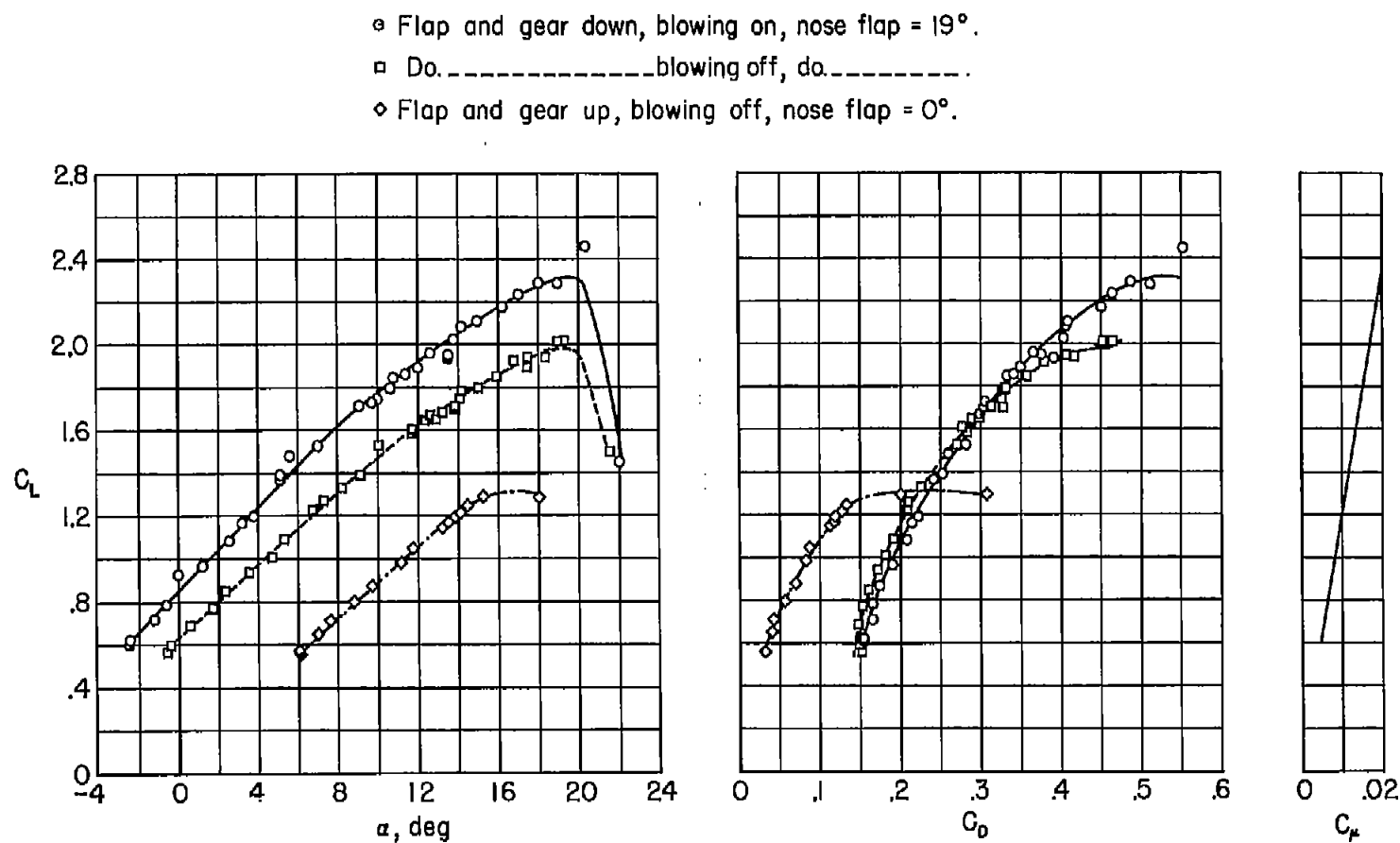
(d) Bleed-air variation with engine speed; valve open.

Figure 4.- Concluded.



A-19986

Figure 5.- Close up of wing showing external hinges and pylons.



(a) Lift characteristics.

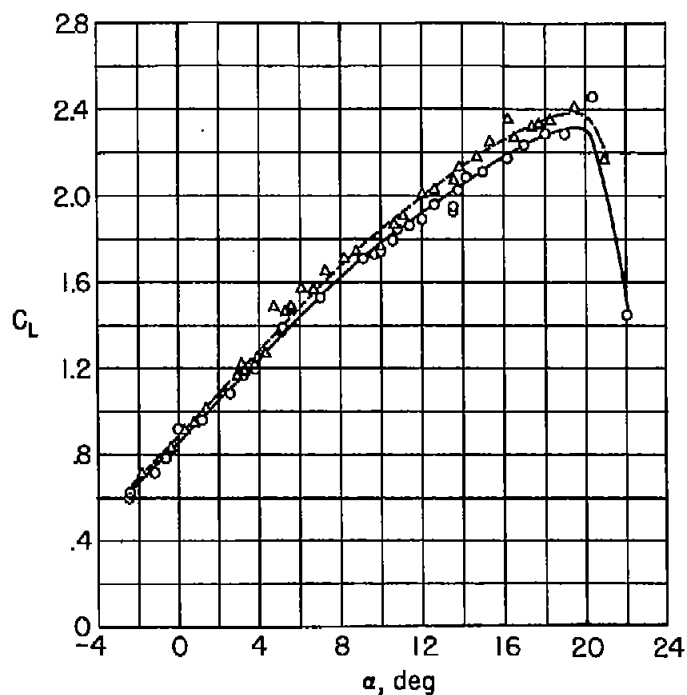
(b) Drag characteristics.

(c) Momentum coefficient.

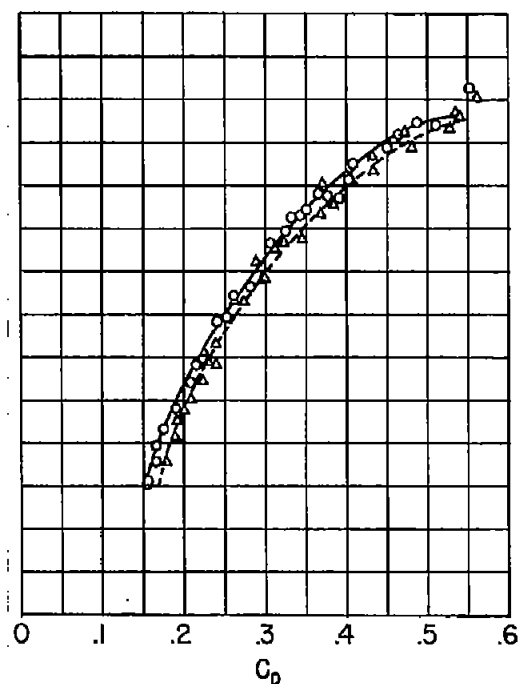
Figure 6.- Lift and drag characteristics of the test airplane; pylons off, approach power $N = 85$ percent.

○ Flap and gear down, blowing on, $N = 85\%$, nose flap = 19° .

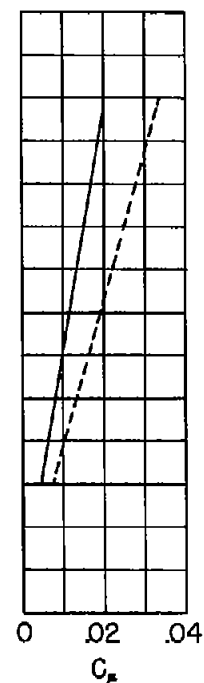
△ Do. ----- $N = 100\%$, do. -----



(a) Lift characteristics



(b) Drag characteristics.



(c) Momentum coefficient.

Figure 7.- The effect of changing engine speed on the lift and drag characteristics of the test airplane; pylons off.

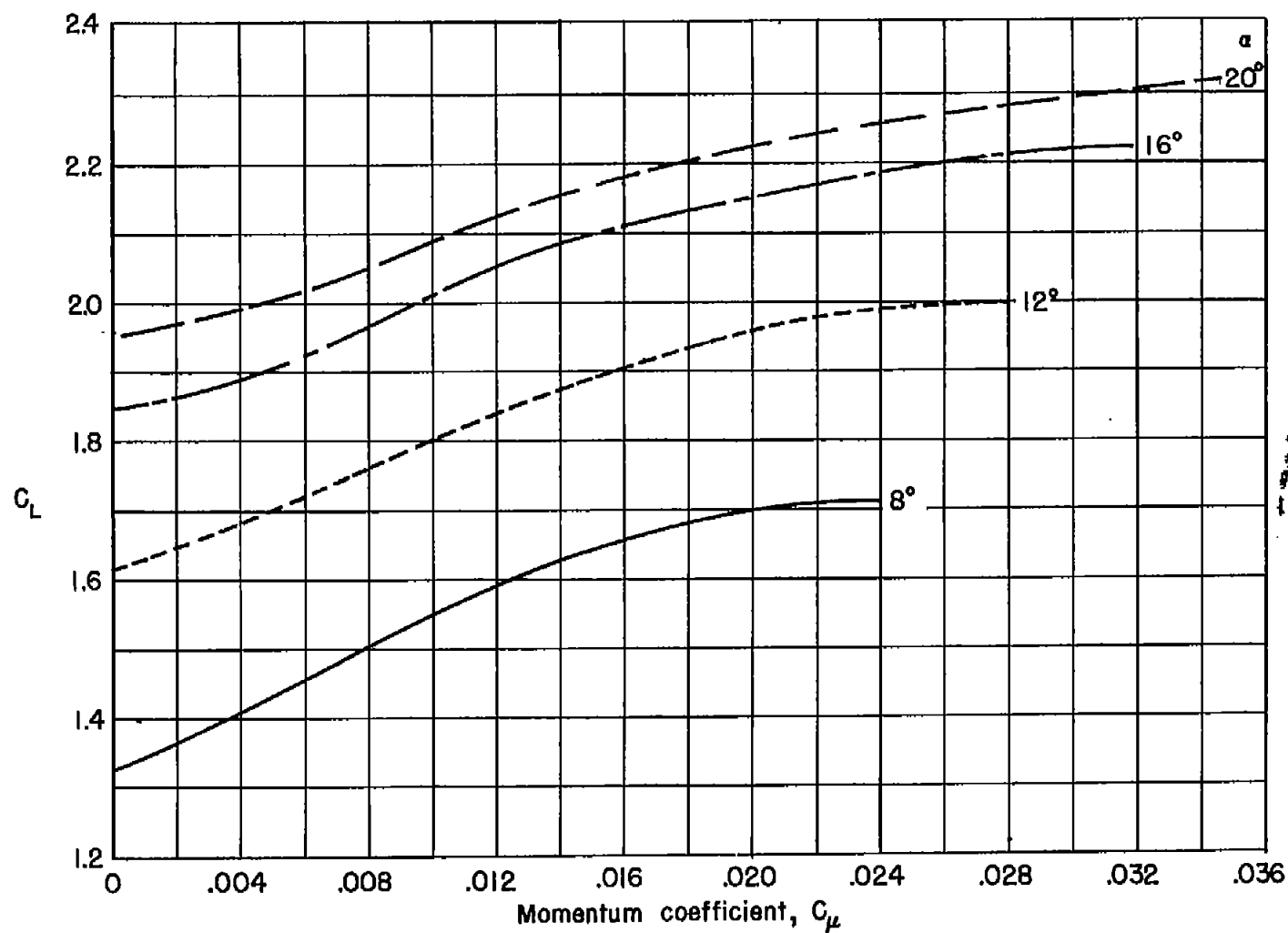


Figure 8.- Variation of lift coefficient with momentum coefficient at several values of angle of attack; test airplane, flap and gear down, nose drooped 19° .

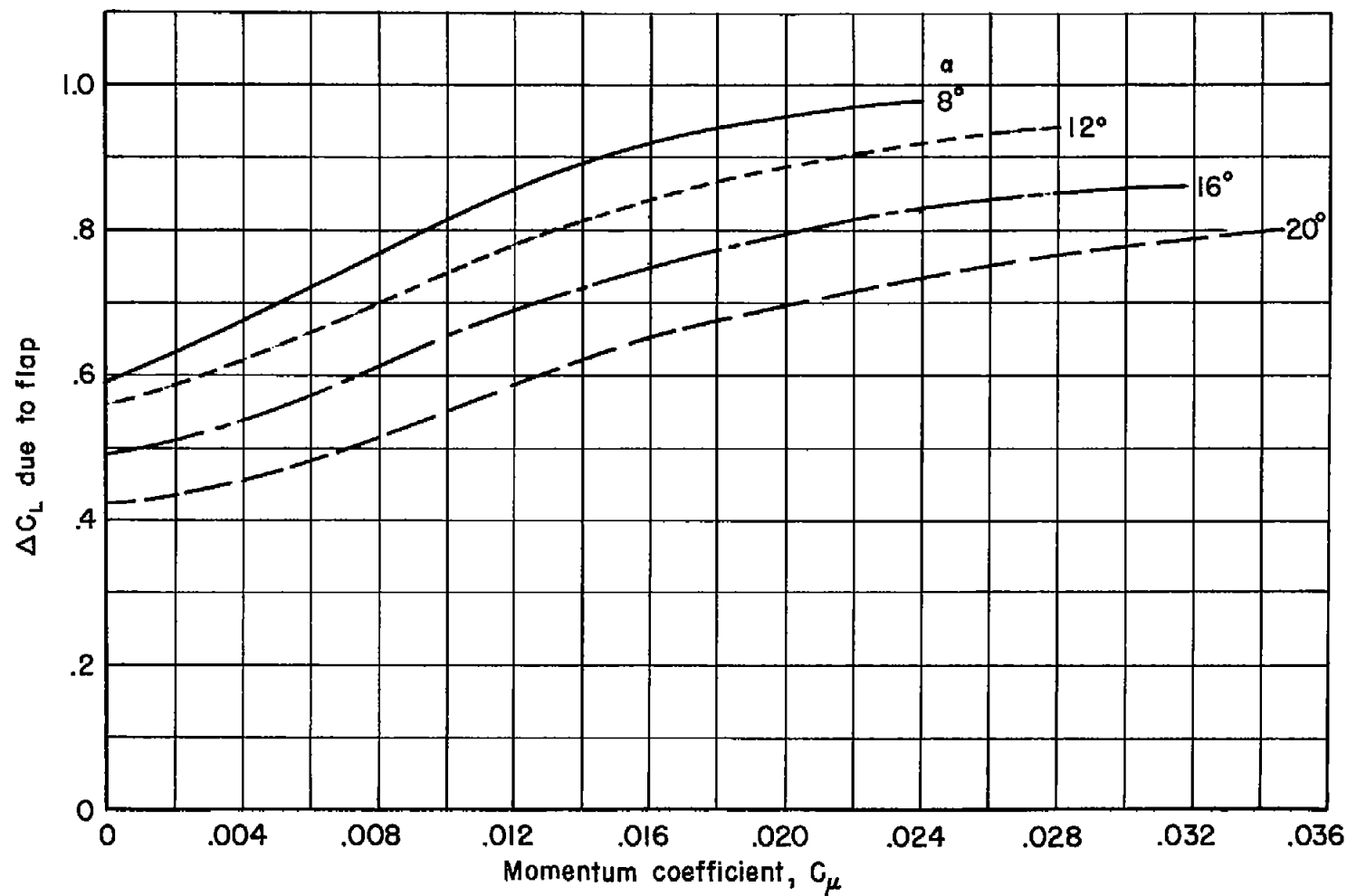


Figure 9.- The variation in flap lift increment caused by increases in momentum coefficient at several angles of attack; test airplane, gear down and nose flap drooped 19° .

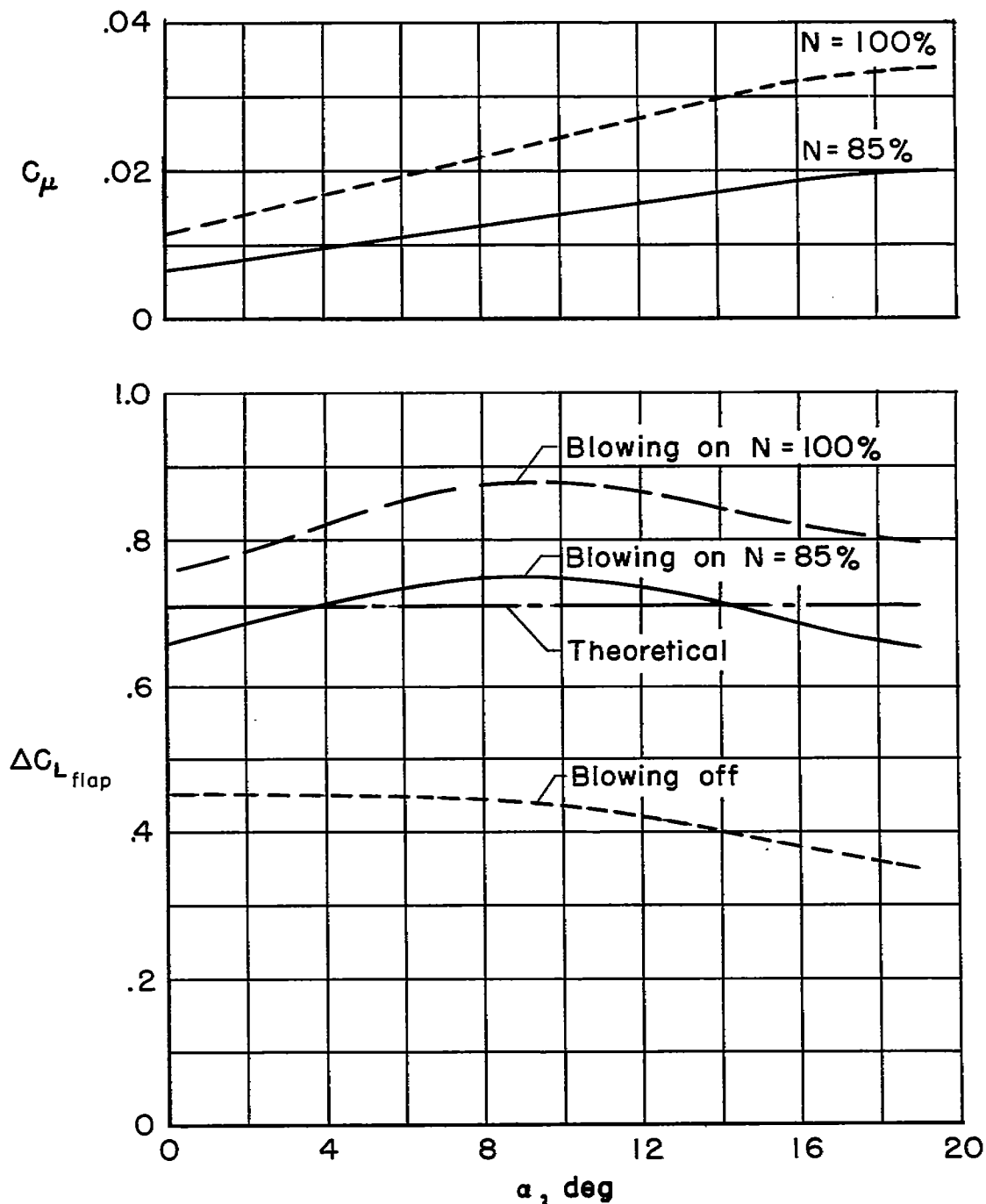


Figure 10.- Variation of flap effectiveness with angle of attack for outboard flap only; tip tanks removed, gear down and nose flap drooped 19° .

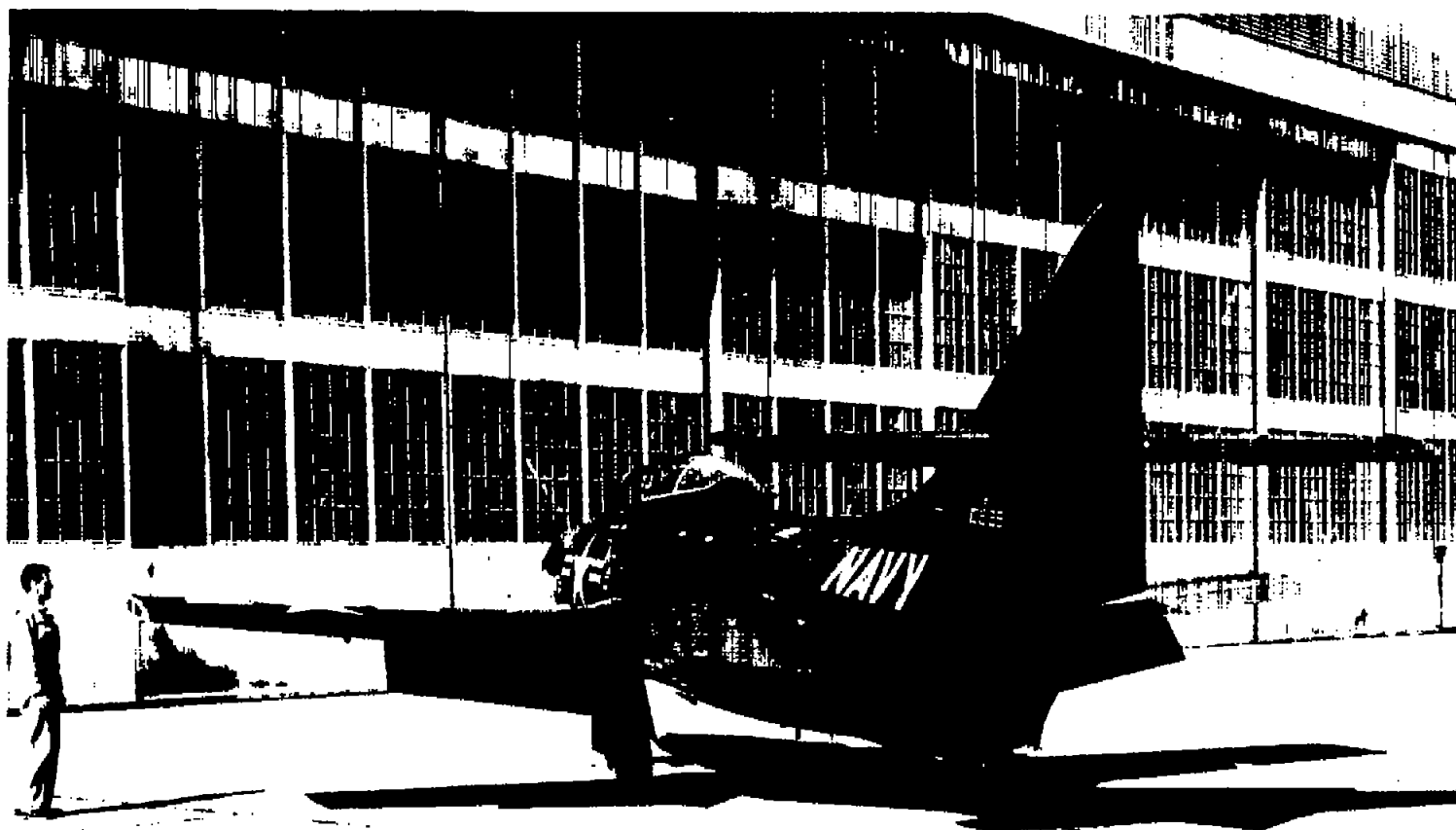


Figure 11.- Three-quarter rear view of test airplane with wing tip tanks removed and outboard flap deflected.

A-20173

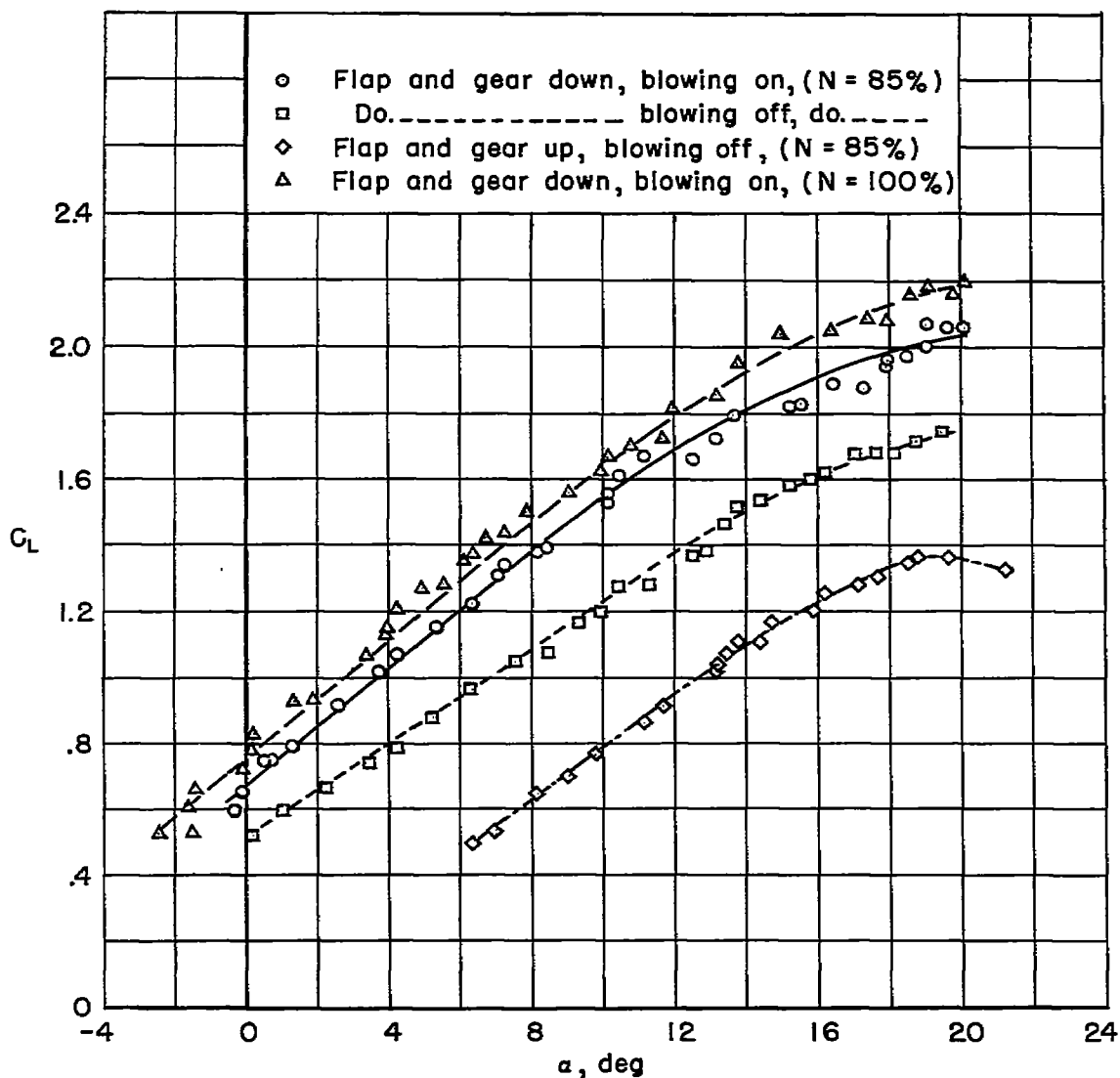
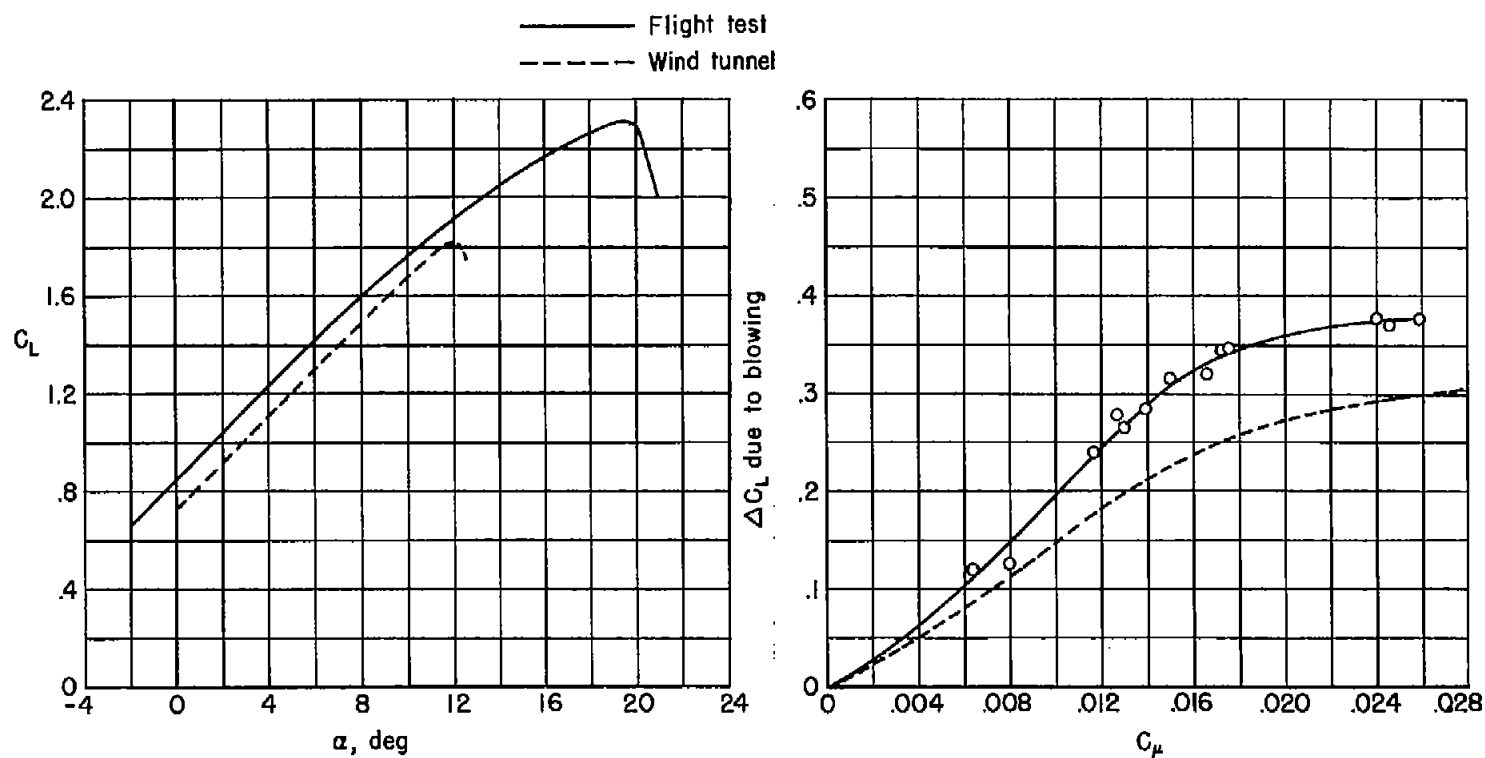


Figure 12.- Variation of lift coefficient with angle of attack; outboard flaps only, wing tip tanks removed, and nose flap drooped 19° .



(a) Variation of lift coefficient with angle of attack in approach condition; $N = 85$ percent, blowing on, nose flap drooped 19° .

(b) Comparison of blowing effectiveness; $\alpha = 10^\circ$.

Figure 13.- Comparison of the flight-test results with test of a 1/5.5-scale model in a wind tunnel (ref. 3).

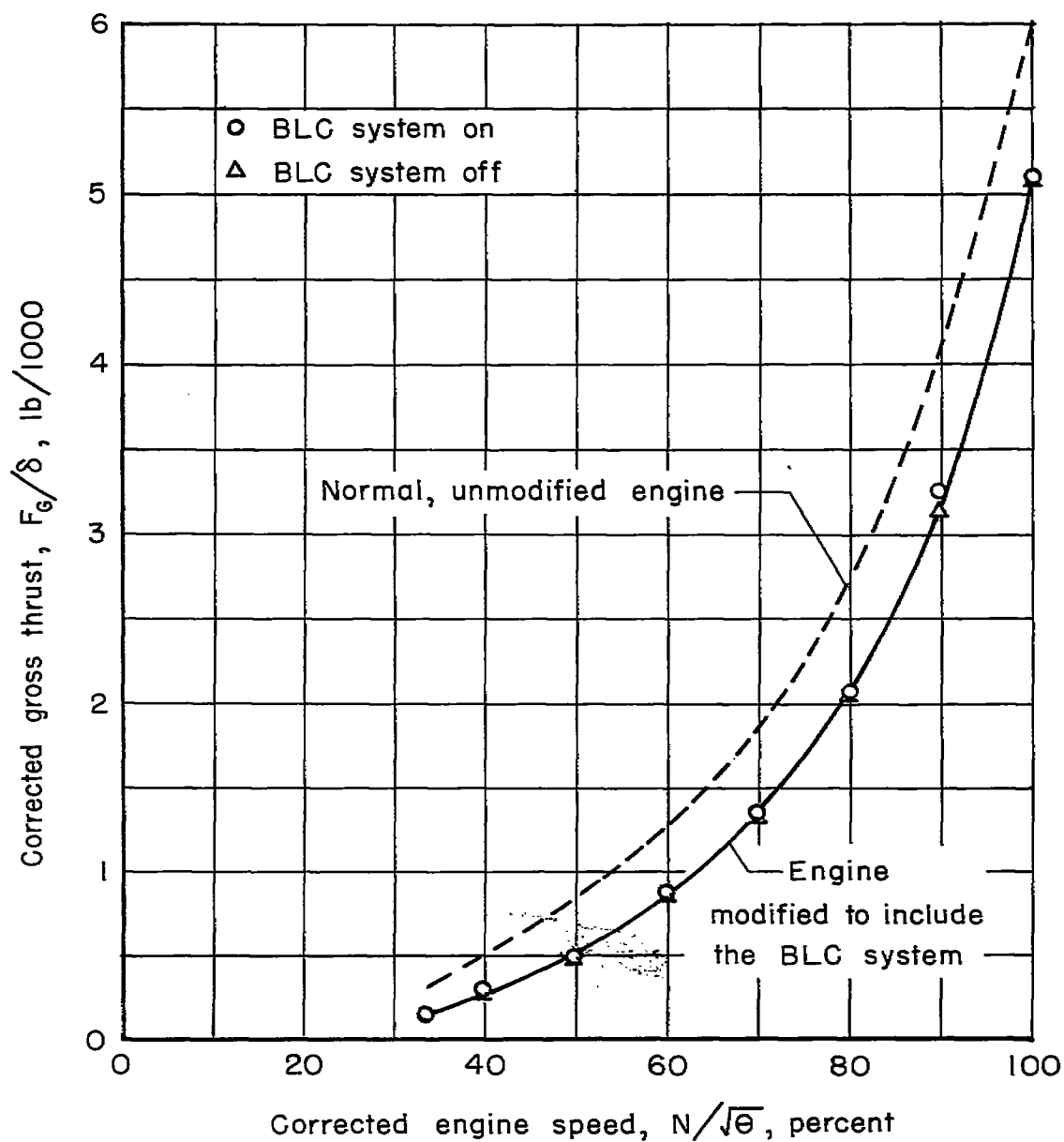


Figure 14.- Comparison of the engine thrust with and without the boundary-layer control system (ref. 6).

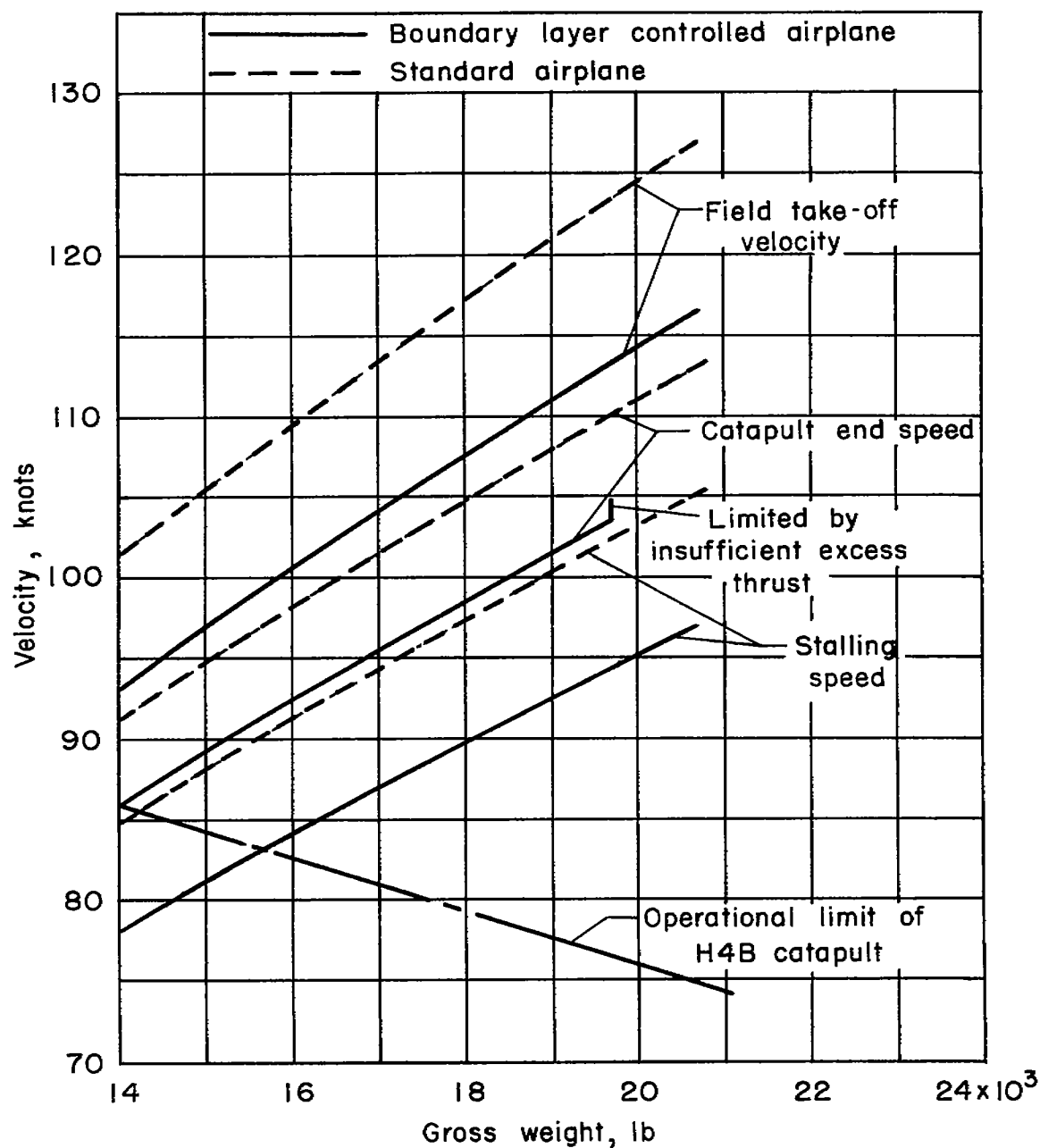


Figure 15.- Comparison of the take-off characteristics of the airplane with boundary-layer control and the standard airplane ($N = 100$ percent).

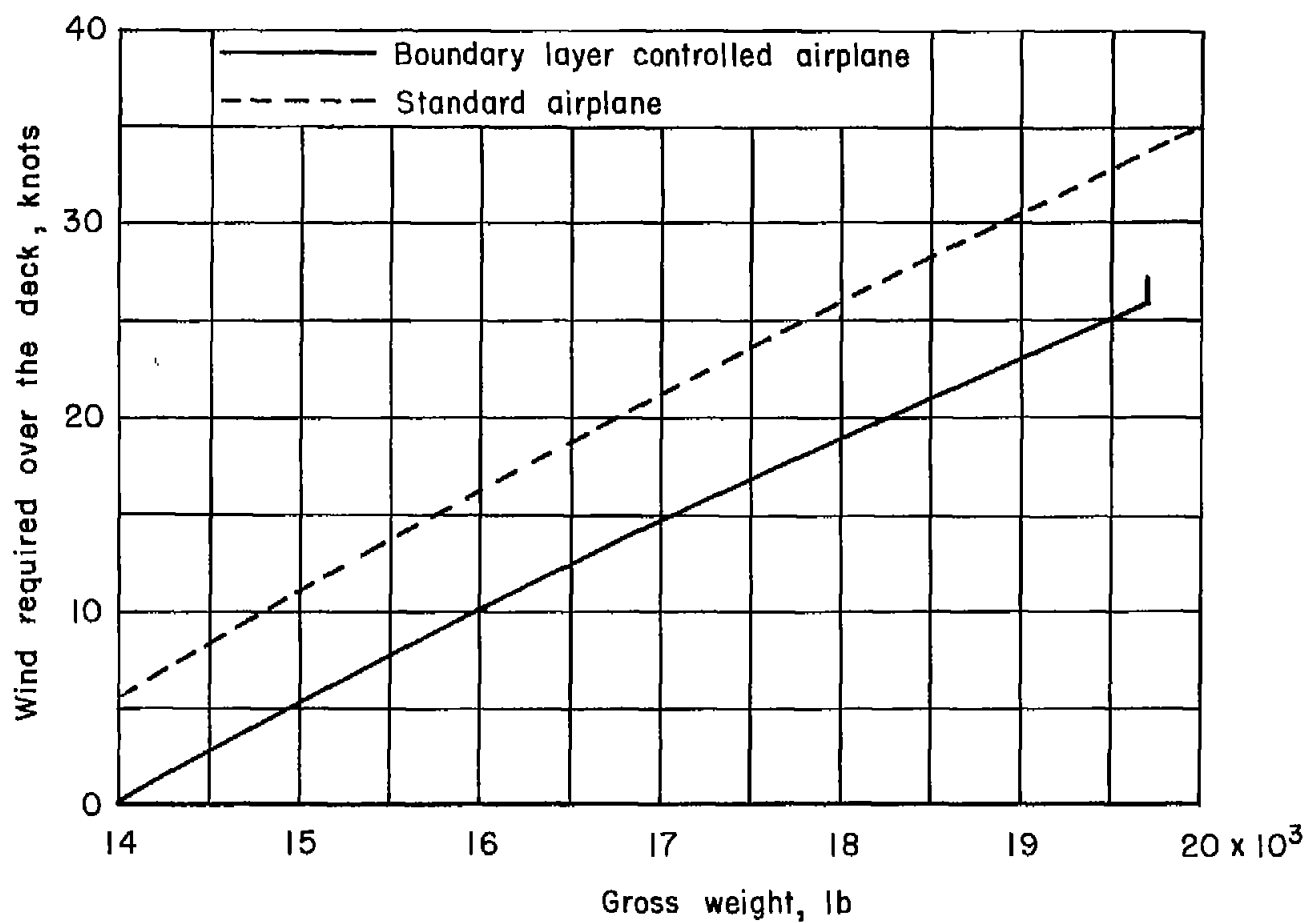


Figure 16.- Comparison of the wind required to catapult the airplane with boundary-layer control and the standard airplane.

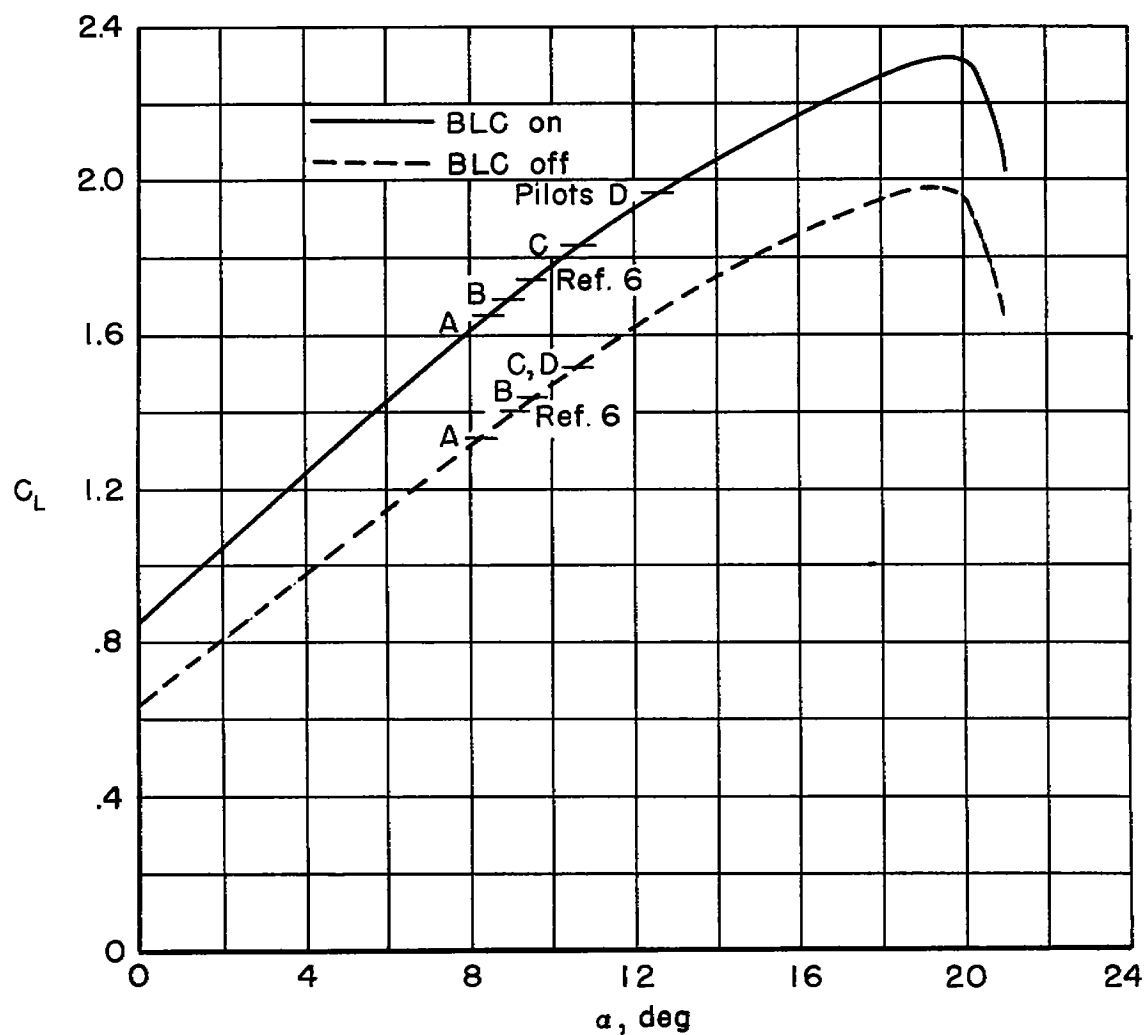


Figure 17.- Approach lift coefficients selected by the Ames research pilots (N = 85 percent).

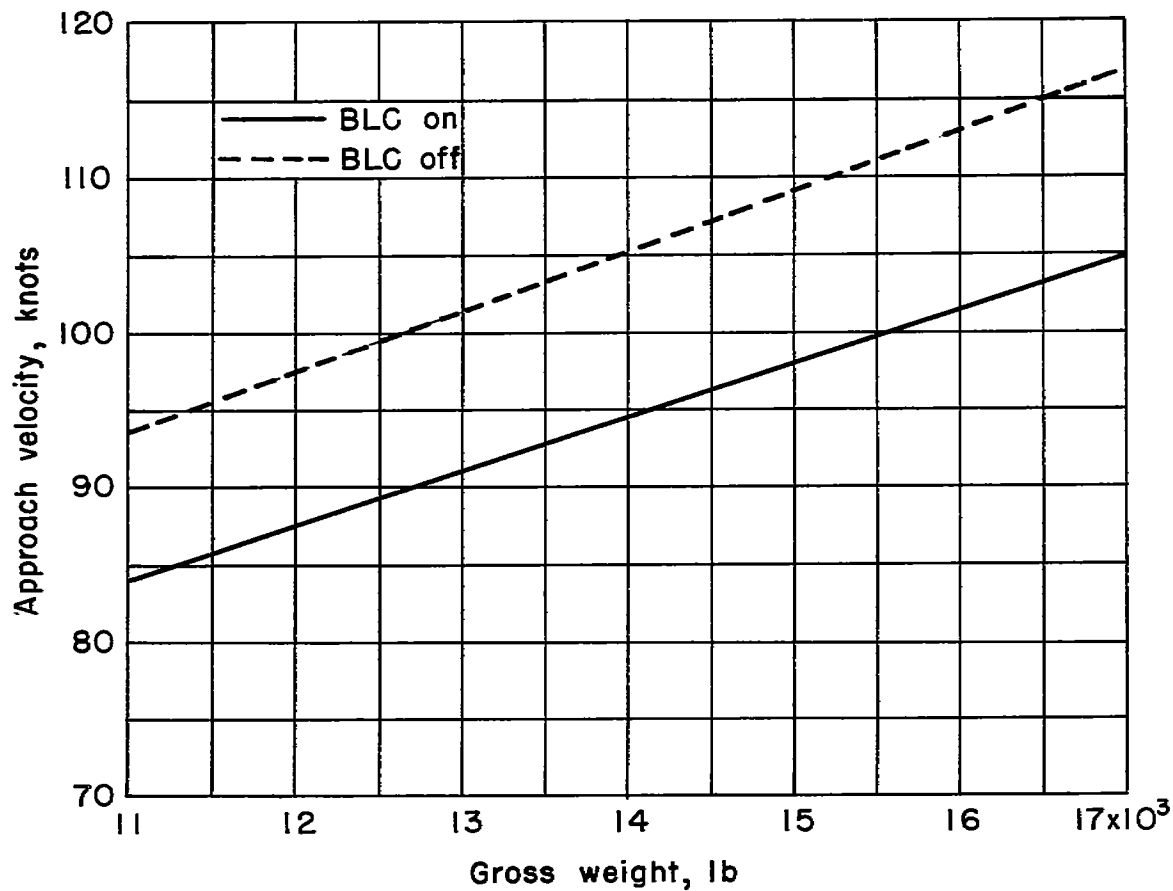


Figure 18.- Variation of approach velocity with gross weight.

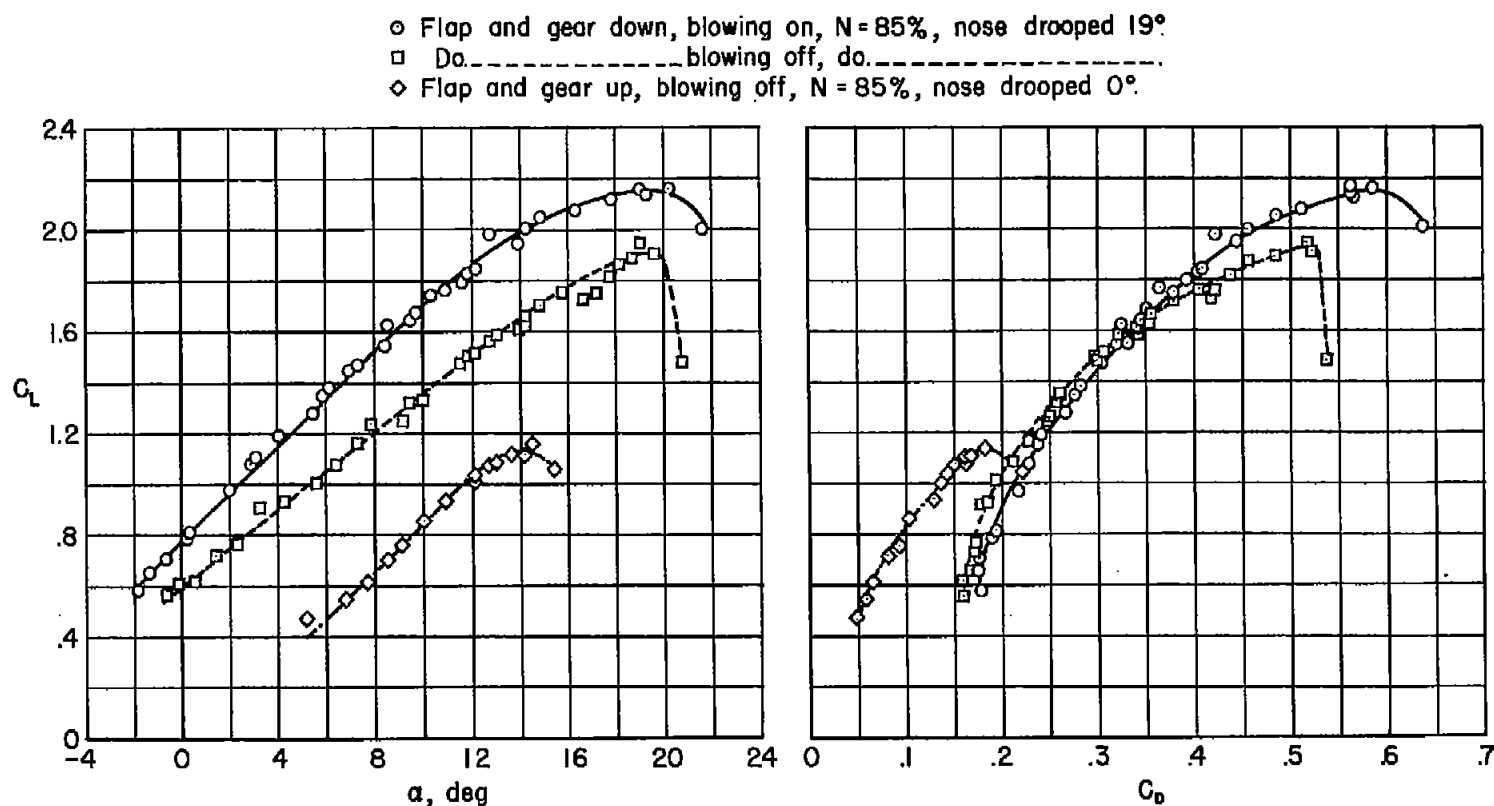
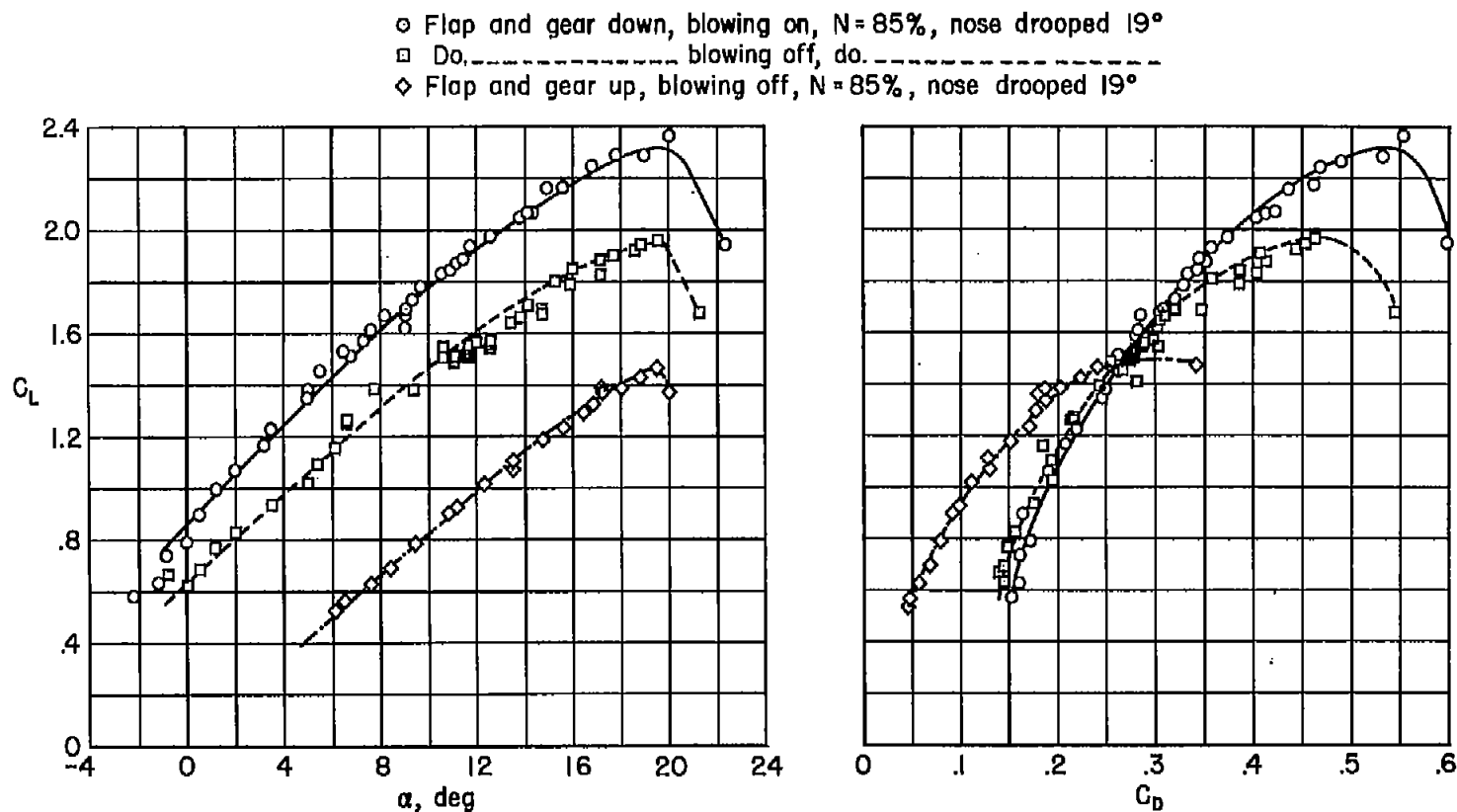


Figure 19.- Lift and drag characteristics of the test airplane with pylons on.



(a) Lift characteristics.

(b) Drag characteristics.

Figure 20.- Lift and drag characteristics of the test airplane with both flaps actuated, nose flap drooped, and pylons on.

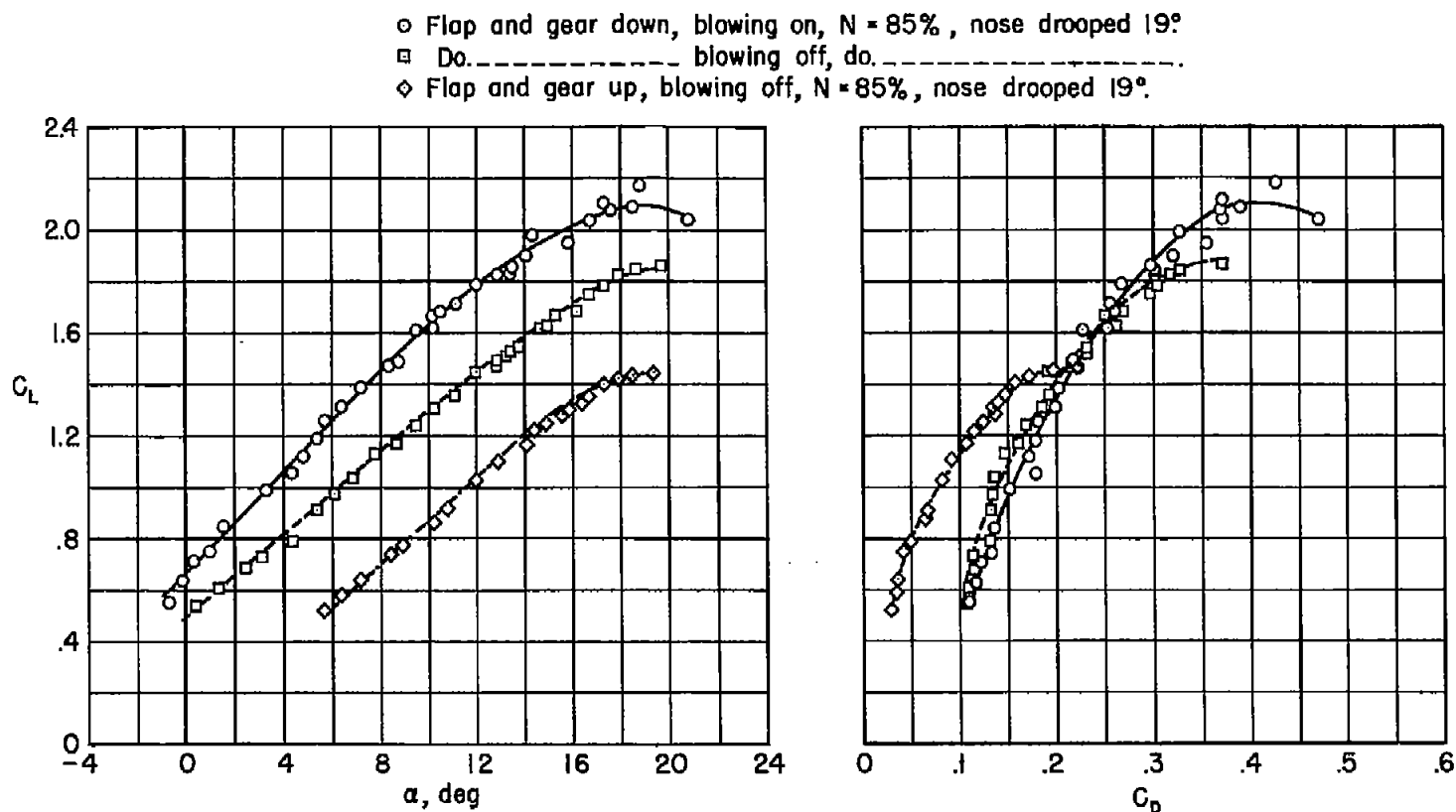


Figure 21.- Lift and drag characteristics of the test airplane with only the outboard flap actuated, nose flap drooped, and pylons off.

14-00000

RESEARCH

THE UNIVERSITY OF CHICAGO PRESS